



Title: Wind Turbine Propulsion of Boats and Ships	Delivered: 09.06.2010
	Availability: Open
Student: Eirik Bøckmann	Number of pages: 69 + Appendices

Abstract:

Increasing focus on reduction of CO₂ emissions, and the possibility of future severe shortage of oil have sparked renewed interest in wind as supplementary propulsion of merchant ships. Several alternative solutions are considered, like kites, conventional soft sails, rigid sails, Flettner rotors, and wind turbines. A tempting aspect of wind turbine propulsion is that it can provide propulsive force when sailing directly upwind, something that is impossible with the other mentioned forms of wind-assisted propulsion.

A method based on axial momentum theory has been outlined, in order to predict the steady-state speed of a wind turbine powered boat. This method is applied to a notional wind turbine powered catamaran. The predicted boat speed to wind speed ratio when the boat is sailing upwind is in good agreement with results from testing of a similar, but smaller, full-scale wind turbine boat.

A related topic to wind turbine propulsion is the reversed configuration, where a water turbine is driving an air propeller. This configuration allows for the theoretical possibility of sailing faster than the wind, directly downwind. Based on a similar approach to the method of velocity prediction of wind turbine powered boats, design criteria with respect to water turbine efficiency and hydrofoil chord length, are set for a given hydrofoil boat in order to sail faster than the wind, directly downwind.

The design of optimal wind turbine blades for wind turbine powered vessels is studied. A 326 m L_{WL} VLCC is equipped with a Vestas V90 wind turbine for auxiliary propulsion, and set to sail a route across the North Sea. By employing the wind turbine, 3.6% of the fuel is saved when the ship is sailing at 15 kn. If the ship speed is reduced to 10 kn, the fuel saving increases to 21.1%. The optimal blade design theory is applied to the wind turbine ship, keeping the wind turbine diameter fixed at 90 m. The optimal blade design increases the fuel saving by a few percentage points. The main drawbacks for a wind turbine powered ship are shown to be the low ship speed to wind speed ratio in order for wind turbine propulsion to be the preferred form of wind-assisted propulsion, as well as the height of such a ship.

Attached is a CD-ROM containing Matlab files used for creating various of the results in this thesis, as well as an electronic version of the thesis.

Keywords:

Wind turbine propulsion
Blade design
Fuel saving

Advisor:

Sverre Steen



M.Sc. thesis 2010

for

Eirik Bøckmann

Wind turbine propulsion of boats and ships

The increasing oil prices and increased focus on CO₂ emissions has led to a greater focus on energy conservation in the marine industry. One way to decrease ships oil consumption is by using wind assisted propulsion – typically traditional as well as rigid sails, Flettner rotors, and kites. Also wind turbines of different kinds have been proposed. The main benefit of wind turbines relative to other types of wind propulsion, is their potential to propel a ship directly upwind. Wind turbine propulsion was investigated 30-40 years ago, but has seen little or no practical application in the later years. The objective of the work is to determine the potential of wind turbine propulsion of boats and ships.

On this background, the student shall do the following in the master thesis:

1. Give a review of previous work on wind turbine propulsion of ships and boats.
2. Present theory for prediction of the performance of wind propelled ships and boats
3. On this theoretical background point out critical aspects in the design of wind turbine propelled ships and boats.
4. Apply the theory on practical examples to show the potential of wind turbine propulsion of ships.
5. Discuss whether wind turbine propulsion could be an interesting technology for reducing the fuel consumption of merchant vessels.

The candidate should in his report give a personal contribution to the solution of the problem formulated in this text. All assumptions and conclusions must be supported by mathematical models and/or references to physical effects in a logical manner.

The candidate should apply all available sources to find relevant literature and information on the actual problem.

The report should be well organised and give a clear presentation of the work and all conclusions. It is important that the text is well written and that tables and figures are used to support the verbal presentation. The report should be complete, but still as short as possible.

The final report must contain this text, an acknowledgement, summary, main body, conclusions, suggestions for further work, symbol list, references and appendices. All figures, tables and equations must be identified by numbers. References should be given by author and year in the text, and presented alphabetically in the reference list. The report must be submitted in two copies unless otherwise has been agreed with the supervisor.

The supervisor may require that the candidate should give a written plan that describes the progress of the work after having received this text. The plan may contain a table of content for the report and also assumed use of computer resources.



From the report it should be possible to identify the work carried out by the candidate and what has been found in the available literature. It is important to give references to the original source for theories and experimental results.

The report must be signed by the candidate, include this text, appear as a paperback, and - if needed - have a separate enclosure (binder, diskette or CD-ROM) with additional material.

Supervisor : Professor Sverre Steen
Start : 18.01.2010
Deadline : 14.06.2010

Trondheim, 18.01.2010

Sverre Steen
Supervisor

Acknowledgements

I would like to thank my supervisor, Prof. Sverre Steen at the Department of Marine Technology, Norwegian University of Science and Technology, for his guidance during my work on this thesis. His support and our helpful discussions are greatly appreciated.

I would also like to thank Prof. Neil Bose, Director of the National Centre for Maritime Engineering and Hydrodynamics at the Australian Maritime College, for sending me some of his papers on wind turbine powered boats, which I was not able to find elsewhere.

Trondheim, 09.06.2010

Eirik Bøckmann

Nomenclature

Roman letters

A	Wind turbine disk area/wingsail area
a	Wind speed reduction factor
a	Derived quantity, see Eq. 3.12
a'	Wind rotation factor
a_0	Optimal wind speed reduction factor
a_1	Derived quantity, see Eq. 3.16
a_2	Derived quantity, see Eq. 3.17
$A_{boat,air}$	Frontal projected area above the waterline for a boat
A_E	Water propeller expanded blade area
$A_{mast,covered}$	Projected area of mast, covered by the wind turbine
$A_{mast,uncovered}$	Projected area of mast, uncovered by the wind turbine
A_p	Disk area of water propeller
A_p	Projected area of the hydrofoil in the direction of the lift
$A_{p,a}$	Disk area of air propeller
A_t	Disk area of wind turbine
$A_{t,w}$	Disk area of water turbine
Asp	Hydrofoil aspect ratio
B	Center of buoyancy
b	Derived quantity, see Eq. 3.13
b	Derived quantity, see Eq. 5.14
c	Chord length of propeller/turbine blade/hydrofoil
c	Derived quantity, see Eq. 3.24
c'	Estimated chord length of hydrofoil
C_D	Drag coefficient of blade element/hydrofoil/wingsail
c_d	Sectional drag coefficient
$C_{D,boat,air}$	Drag coefficient of boat above the waterline
C_{Di}	Induced drag coefficient of hydrofoil
$C_{D,mast}$	Drag coefficient of mast
C_{Dv}	Viscous drag coefficient of hydrofoil
C_F	Skin friction coefficient
C_L	Lift coefficient of blade element/hydrofoil/wingsail
c_l	Sectional lift coefficient
C'_L	Estimated lift coefficient of blade element
C_P	Power coefficient of wind turbine
C_T	Thrust coefficient of wind turbine
C_T	Total resistance coefficient

D	Water propeller diameter
d	Derived quantity, see Eq. 3.25
$EAR = A_E/A_p$	Expanded area ratio of propeller
E_{tot}	Total energy consumed over the journey
F	Water/air propeller thrust
f	Boat speed to wind speed ratio
F_0	Ideal thrust, zero speed
F_D	Water resistance on the boat
F_D	Drag force on wingsail
F_{Da}	Air resistance on the boat excluding the wind turbine
F_L	Lift force on wingsail
$F_{net} = F - F_W$	Force available to overcome water and air resistance of boat/ship
F_W	Force on the wind/water turbine in the direction of the boat course
G	Center of gravity, hydrostatics
GZ	Righting arm, hydrostatics
g	Gravitational acceleration
$H(s)$	Derived quantity, see Eq. 4.13
h_G	Distance from deck to center of gravity
$h_{mid,covered}$	Middle height above deck of the part of the mast that is covered by the wind turbine
$h_{mid,uncovered}$	Middle height above deck of the part of the mast that is uncovered by the wind turbine
h_t	Hub height above deck
$J = \frac{V_A}{nD}$	Propeller advance number
K	Keel
K_T	Propeller thrust coefficient
K_Q	Propeller torque coefficient
L	Lift of hydrofoil
L'	Estimated lift of hydrofoil
L_{pp}	Length between perpendiculars
L_R	Sound pressure level of noise at distance R from the noise source
L_W	Sound power level of noise source
L_{WL}	Length on waterline
\dot{m}	Mass flow rate of fluid
M	Metacenter
$M_{heeling}$	Heeling moment
$M_{righting}$	Righting moment

N	Number of propeller/turbine blades
n	Propeller revolution speed in rps
P	Power from wind/water turbine/propulsive power from propeller
P	Propeller pitch
P_D	Power delivered to the propeller
P_i	Ideal power required to drive the propeller
p_0	Pressure in the propeller/turbine freestream, momentum theory
p_1	Pressure in front of the propeller/turbine, momentum theory
p_2	Pressure behind the propeller/turbine, momentum theory
Q	Volume flow through the propeller/turbine disk
Q	Propeller/turbine torque
R	Wind turbine radius
R	Distance between sound source and receiver
Re	Reynold's number
r	Radial propeller/turbine blade position
S	Wetted surface of boat
$S = \frac{\Omega R}{U}$	Tip speed ratio
$s = \frac{\Omega r}{U}$	Speed ratio
s	Span of hydrofoil
T	Thrust on wind turbine
U	Apparent wind speed with respect to boat
u	Boat speed
$\bar{U}(z)$	Mean wind speed at elevation z
\bar{U}_{10}	Mean wind speed at 10 m elevation
$u_e = u + \Delta u$	Velocity behind propeller disk, momentum theory
u_p	Velocity through propeller disk, momentum theory
U_t	Velocity through turbine disk, momentum theory
V	Apparent wind speed experienced by rotating blade element
V_A	Propeller advance velocity
W	Wind speed
z	Height above ground/water

Greek letters

α	Wind turbine blade element angle of attack
α	Coefficient in Eq. 5.9

α_a	Attenuation of sound due to air absorption
Γ	Circulation
ΔL_a	Sound reduction in air in Eq. 5.20
Δp	Pressure difference across turbine disk, momentum theory
ΔU	Wind velocity loss due to wind turbine
ΔU	Wind velocity gain to air propeller
Δu	Water velocity loss due to water turbine
Δu	Water velocity gain due to water propeller
$\epsilon = C_D/C_L$	Drag-to-lift ratio
$\zeta = \eta_p \eta_g$	Overall efficiency of driving mechanism
η_0	Open water efficiency
η_g	Gearing/transmission efficiency
$\eta_{i,a}$	Inviscid efficiency of air propeller
η_p	Water propeller efficiency
$\eta_{p,0}$	Water propeller efficiency at zero advance velocity
$\eta_{p,a}$	Air propeller efficiency
$\eta_{swirl,a}$	Swirl efficiency of air propeller
η_t	Wind turbine efficiency
$\eta_{t,w}$	Water turbine efficiency
$\eta_{t,w,2} = \frac{P}{F_W u}$	Another definition of water turbine efficiency
$\eta_{v,a}$	Viscous efficiency of air propeller
θ	Angle between true wind and boat course
θ'	Apparent wind angle with respect to boat course
ρ_a	Mass density of air
ρ_w	Mass density of water
ϕ	Apparent wind angle with respect to blade element
ϕ	Heel angle
Ω	Wind turbine rotation rate in rad/s

Abbreviations and acronyms

DAWT	Diffuser-Augmented Wind Turbine
DDFTTW	Directly Downwind Faster Than The Wind
HAWT	Horizontal-Axis Wind Turbine
ITTC	International Towing Tank Conference
RANS	Reynolds-Averaged Navier Stokes
VAWT	Vertical-Axis Wind Turbine
VLCC	Very Large Crude Carrier

Contents

Acknowledgements	i
Nomenclature	ii
1 Introduction	1
1.1 Background and motivation	1
1.2 Previous work	3
2 Velocity predictions for a wind turbine powered boat	5
2.1 Introduction	5
2.2 Modes of operation	5
2.3 Michlet model	6
2.4 Velocity prediction method	8
3 Directly Downwind Faster Than The Wind?	18
3.1 Introduction	18
3.2 Velocity prediction	19
3.3 Propeller efficiency	22
3.4 Overcoming drag at the wind speed	23
3.5 Designing the boat to go DDFTTW	26
4 Optimization of the wind turbine powered boat	30
4.1 Blade element theory	30
4.2 Optimal apparent wind angle distribution	33
4.3 Optimal blade chord distribution	36
4.4 Correction for a finite number of blades	37
5 Use of wind turbines on ships	40
5.1 What type of wind turbine?	40
5.2 Comparison against other forms of wind-assisted ship propulsion	44
5.3 Fuel savings for a notional wind turbine ship	47
5.4 Optimized notional wind turbine ship	54
5.5 Considerations on a wind turbine propelled ship	58
6 Conclusions and future perspectives	63
6.1 Conclusions	63
6.2 Future perspectives	65
References	67
Appendix A Momentum theory	70
A.1 Momentum theory, wind turbine	70
A.2 Momentum theory, propeller	72
A.3 Propeller efficiency at zero speed	73
Appendix B Resistance and hydrostatics results, ShipX	75

List of Figures

Figure 1.1	Wind turbine boats built for research (Bose, 2008).	2
Figure 1.2	More examples of wind turbine boats (Bose, 2008).	3
Figure 1.3	<i>Revelation II</i>	4
Figure 2.1	Modes of operation. Modified from (Bose, 2008).	6
Figure 2.2	Michlet model.	7
Figure 2.3	Water resistance found with Michlet.	8
Figure 2.4	Sketch of a windmill boat (catamaran) sailing upwind. Modified from (Blackford, 1985a).	9
Figure 2.5	Sketch of wind and boat velocity vectors (Blackford, 1985a).	9
Figure 2.6	Relation between Eq. 2.6 and Betz limit.	11
Figure 2.7	Open water diagram.	12
Figure 2.8	K_Q/J^3 vs J	13
Figure 2.9	Thrust vs resistance, $\theta = 0^\circ$	14
Figure 2.10	Water propeller efficiency, $\theta = 0^\circ$	15
Figure 2.11	Water propeller diameter vs f , $\theta = 0^\circ$	16
Figure 2.12	Thrust vs resistance, $\theta = 90^\circ$	16
Figure 2.13	Thrust vs resistance, $\theta = 180^\circ$	17
Figure 2.14	Boat speed to wind speed ratio vs true wind angle.	17
Figure 3.1	The original and a modern full-scale DDFTTW cart.	19
Figure 3.2	Apparent velocities, DDFTTW. Modified from (Drela, 2009a).	20
Figure 3.3	Different flow regimes of a propeller. Modified from (Bauer, 1969).	21
Figure 3.4	a_2 as a function of water turbine diameter and $\eta_{t,w}$	26
Figure 3.5	a_1 for a hydrofoil boat.	28
Figure 4.1	Wind turbine blade element with air velocity compo- nents (Blackford, 1985a).	31
Figure 4.2	The value of $a(s)$ that maximizes F_{net}	33
Figure 4.3	Influence of choice of $a(s)$ on the dimensionless net force.	34
Figure 4.4	Apparent wind angle ϕ vs true wind angle θ	35
Figure 4.5	Chord distribution.	37
Figure 4.6	Goldstein factors for four-bladed propellers. Modified from (Carlton, 2007).	38
Figure 5.1	Different suggestions for windmill ships (Bose, 1980).	40
Figure 5.2	Three different types of VAWTs.	41
Figure 5.3	Diffuser-Augmented Wind Turbine (Wind-Works, 2010).	41
Figure 5.4	Ideal flow through a wind turbine in a diffuser (Hansen, 2008).	42

Figure 5.5	Computed power coefficient C_p for a rotor in a diffuser as a function of the thrust coefficient C_T (Hansen, 2008).	43
Figure 5.6	Normalized net forward force versus true wind angle, θ , for wingsail and wind turbine propulsion, $f = 0.5$. Modified from (Blackford, 1985a).	45
Figure 5.7	Normalized net forward force versus true wind angle, θ , for wingsail and wind turbine propulsion, $f = 0.75$. Modified from (Blackford, 1985a).	45
Figure 5.8	Fuel power required for ships with wind rigs. Modified from (Nance, 1985; Rainey, 1980).	46
Figure 5.9	The route for the wind turbine ship.	48
Figure 5.10	Vestas V90 power curve (Vestas, 2009).	50
Figure 5.11	Vestas V90 efficiency.	50
Figure 5.12	Net power from a Vestas V90 wind turbine for a ship sailing at 15 kn.	51
Figure 5.13	Blade chord distribution for the optimized wind turbine ship.	55
Figure 5.14	Blade pitch angle distribution, $\phi - \alpha$, for the optimized wind turbine ship.	55
Figure 5.15	F_{net} as a function of ζ . $\theta = 0$, $W = 10$ m/s, and $f = 0.5$.	58
Figure 5.16	Heeling ship with heights explained.	59
Figure 5.17	Ship stability notation.	60
Figure 5.18	Heeling and righting moments in 12.5 m/s beam wind, zero ship speed.	60
Figure A.1	Axial momentum theory, wind turbine.	70
Figure A.2	Axial momentum theory, propeller.	72
Figure B.1	Resistance curve for the VLCC from ShipX.	75

List of Tables

Table 2.1	Main dimensions of the catamaran analyzed.	7
Table 3.1	Chord length of hydrofoil for a DDFTTW boat.	29
Table 4.1	Optimal wind turbine rotation rate.	36
Table 4.2	Influence of Prandtl and Goldstein corrections on blade design.	38
Table 4.3	Influence of Prandtl's tip loss factor on wind turbine performance.	39
Table 5.1	Wind-assisted propulsion performance envelope chart (Bose, 2008).	47
Table 5.2	Route with wind data (Windfinder, 2010).	48
Table 5.3	Main dimensions of the wind turbine ship.	49

Table 5.4	Vestas V90 key data.	50
Table 5.5	Energy savings for the North Sea route at 15 kn.	52
Table 5.6	Energy savings for the North Sea route at 10 kn.	53
Table 5.7	Design parameters for the optimized wind turbine ship.	57

1 Introduction

1.1 Background and motivation

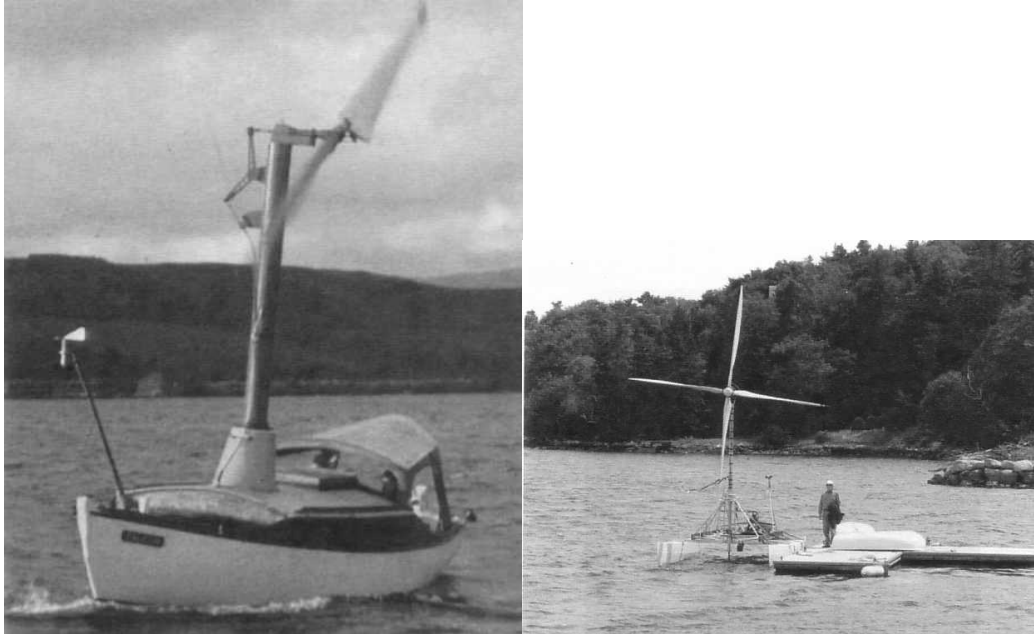
Increasing focus on reduction of CO₂ emissions, and the possibility of future severe shortage of oil have sparked renewed interest in wind as supplementary propulsion of merchant ships. Several alternative solutions are considered, like kites, conventional soft sails, rigid sails, Flettner rotors, and wind turbines. A tempting aspect of wind turbine propulsion is that it can provide propulsive force when sailing directly upwind, something that is impossible with the other mentioned forms of wind-assisted propulsion. In the literature, and also in this thesis, the words windmill and wind turbine are both used in conjunction with propulsion, regardless of the way the windmill or wind turbine is connected to the water propeller - mechanically, electrically or hydraulically.

The idea of using a windmill to mechanically drive the water propeller of a boat is far from new. A windmill-powered vessel design was proposed in 1712 in France for invading England, and the wind turbine-propelled boat *Bois Rosé* was produced by the French engineer Constantin in 1924 (Bose, 2008). In 1933, Lt Col J. T. C. Moore-Brabazon, later Lord Brabazon, built a boat equipped with a wind turbine rotor which did not drive a propeller, but instead worked as an autogyro providing direct aerodynamic thrust (Rainey, 1980).

The interest in windmill boats, or wind turbine boats, boosted in the 1980s, as a result of the 1979 oil crisis which inspired naval architects and engineers to evaluate various forms of wind propulsion for commercial ships. Research on wind turbine boats were conducted mainly at Glasgow University by Neil Bose, and at Dalhousie University by Brad Blackford. Both Blackford's and Bose's research included testing of full-scale wind turbine boats, which documented that wind turbine boats could indeed sail straight into the wind, a feature which many people find "unphysical" at first thought.

Several wind turbine boats were built in the 1980s, but as the oil price dropped in the latter part the decade, the interest in the wind turbine boat gradually faded. More recently, Jim Wilkinson's 36-foot catamaran *Revelation II* of 2001, see Fig. 1.3, has sparked renewed interest in wind turbine

boats. *Revelation II* carries a wind turbine with three 6.1 m carbon fiber blades, and is reported to sail faster into a headwind, than with the wind behind it (BBC News, 2001).



(a) Neil Bose's *Falcon*

(b) Brad Blackford's wind turbine boat

Figure 1.1: Wind turbine boats built for research (Bose, 2008).

Although many models and full-scale wind turbine boats have been built, no commercial ship has yet been equipped with one or more wind turbines for auxiliary propulsion. Reasons for this are discussed in Sec. 5. As shown in Sec. 5.2, the ship speed to wind speed ratio is of utter importance to the physical feasibility of employing a wind turbine rig on a ship, and the economic effects of increasing transit times should be evaluated against the fuel savings obtained through lower ship speeds.

A related topic to wind turbine propulsion is the reversed configuration, where, instead of a wind turbine driving a water propeller, the water propeller is used as a water turbine to drive an air propeller. Whereas a wind turbine powered vessel will lose its propulsive force when sailing downwind and approaching the wind speed, a vessel with the reversed configuration will, being designed correctly, increase its propulsive force when sailing downwind and approaching the wind speed. The limiting factor to whether or not such a vessel may sail faster than the wind speed, directly downwind, is mainly the water drag, which is discussed in Sec. 3.5.

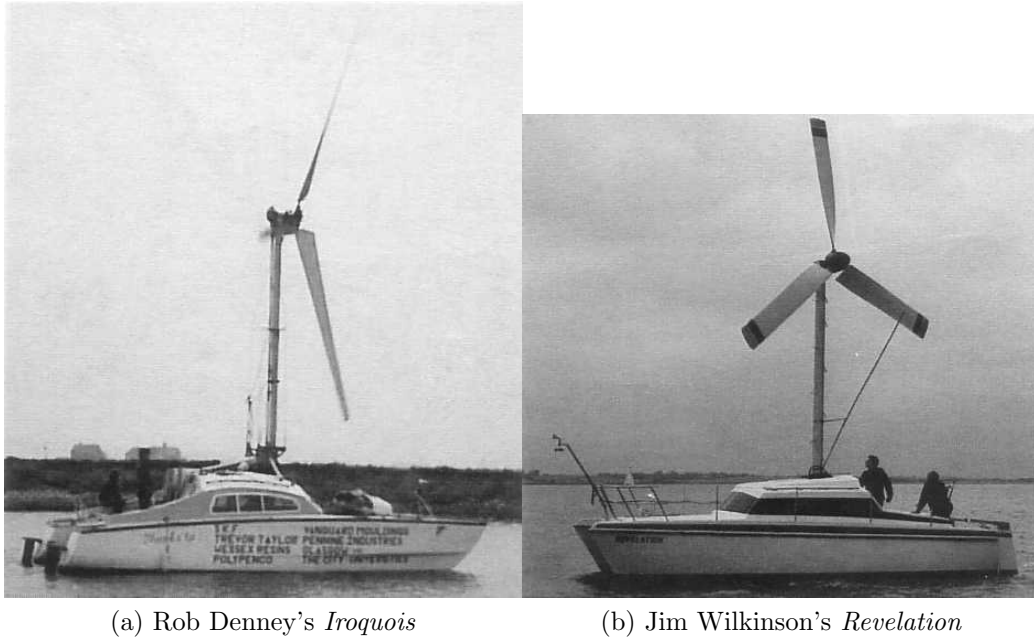


Figure 1.2: More examples of wind turbine boats (Bose, 2008).

1.2 Previous work

The *Symposium on Wind Propulsion of Commercial Ships* arranged by the Royal Institution of Naval Architects (RINA) in November 1980 initiated a small wave of papers on wind turbine propulsion for boats and ships. R. C. T. Rainey's paper *The Wind Turbine Ship* (Rainey, 1980), presented at the Symposium, states that the wind turbine powered ship is “[...] on paper one of the most attractive possibilities [for wind-assisted ship propulsion] among commercial sailing rigs”.

Neil Bose published several papers on wind turbine propulsion in the 1980s, covering aspects such as testing of full-scale wind turbine boats (Bose, 1985), (Bose and Wilkinson, 1985), the autogyro used for ship propulsion (Bose, 1983), and wind turbine propulsion for a Scottish Seiner/Trawler (Bose and MacGregor, 1987). Brad Blackford discusses optimal blade design for wind-mill boats and vehicles in (Blackford, 1985a), and compares theory with experiments in (Blackford, 1985b).

In the paper *Outlook for wind assistance* (Nance, 1985), C. T. Nance evaluates the wind turbine propelled ship against other forms of wind-assisted



Figure 1.3: *Revelation II.*

ship propulsion such as conventional sails, rigid sails, kites and Flettner rotors. In the evaluation, see Fig. 5.8, the wind turbine propelled ship is the most fuel-saving of all the alternatives, when all wind directions are taken into consideration. It should be noted that Nance bases his comparison on Rainey's paper (Rainey, 1980), which calculates auxiliary power required for a wind turbine ship traveling at half the wind speed.

Regarding the configuration where a water turbine is driving an air propeller, A. B. Bauer discusses the theoretical performance of such a vessel in (Bauer, 1969). M. Drela also analyses such a vessel in (Drela, 2009a,b).

2 Velocity predictions for a wind turbine powered boat

2.1 Introduction

Before studying the wind turbine blade design in detail in Sec. 4, a simple procedure is described to determine how fast a given wind turbine powered boat will sail in all wind directions. The force on the wind turbine is calculated using axial momentum theory, see Appendix A.1. It is assumed that the wind turbine efficiency, water propeller efficiency, and transmission efficiency, or gearing efficiency, is known. The theoretical approach is shown for a low drag catamaran hull, 11.5 m long, with a wind turbine diameter of 8 m. It is assumed that the boat has no cabin or structures on deck other than what is necessary to support the wind turbine - it's only purpose is to sail as fast as possible.

A wind turbine efficiency of 0.4 is assumed here for a wind speed of 5 m/s, which may be realistic for a given wind turbine. In order to study the effect of wind speed on the boat speed, without letting the result be affected by varying wind turbine efficiency, a wind turbine efficiency of 0.4 is also used for wind speeds of 10 m/s and 15 m/s. As discussed in Sec. 5.3, however, the wind turbine efficiency is a function of the wind speed, and the boat speed to wind speed ratio will in reality be affected by this.

2.2 Modes of operation

As described in detail in (Bose, 1983), the wind turbine rotor can provide forward thrust on reaching courses if it is spinning freely like an autogyro. This was first shown experimentally in the 1930s, by Lord Brabazon in the UK and Alexander Klemin in the USA, on small boats. Similar to traditional sails, the autogyro provides forward thrust through lift and drag, see Fig. 2.1.

The leeway angle, shown in Fig. 2.1, is the angle between the boat's heading and its actual course, due to wind drift. Bose (Bose, 1983) states that in beam wind, the propulsion force will be larger in the autogyro mode than

in the wind turbine mode, but that the optimal blade design for the rotor in the two modes of operation will be different. The autogyro mode is not studied further here. Instead, optimal blade design of the rotor in the wind turbine mode is studied in Sec. 4.

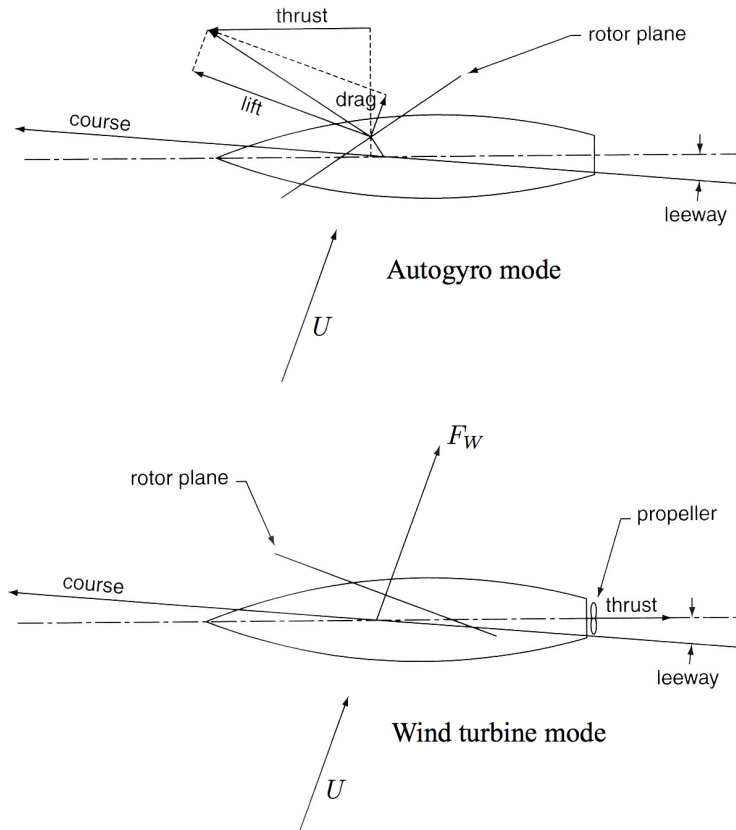


Figure 2.1: Modes of operation. Modified from (Bose, 2008).

2.3 Michlet model

The water resistance of the catamaran is found using the program *Michlet*, available for free at <http://www.cyberiad.net/michlet.htm>. Fig. 2.2 shows the underwater hulls, and the main dimensions of the boat are given in Table 2.1. The catamaran studied is the “Standard Catamaran” example input file named *gcatin.mlt*, in the *GODZILLA* module of *Michlet*. The optimal hull spacing with respect to minimizing the total resistance, is found using *GODZILLA*. Fig. 2.3 shows the total water resistance of the boat for

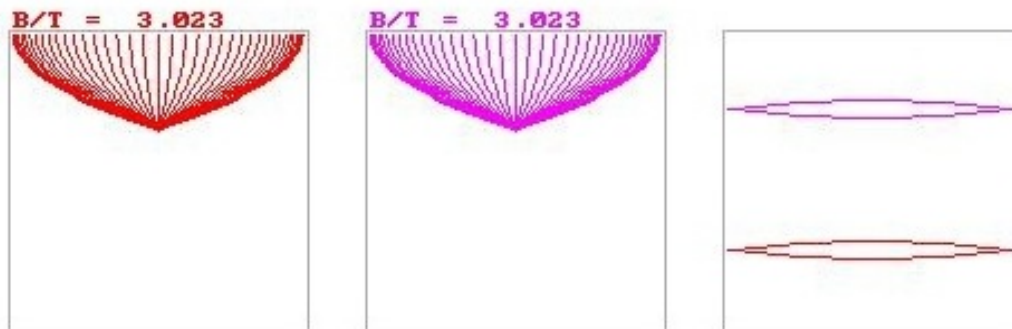


Figure 2.2: Michlet model.

boat speeds up to 11 m/s, calculated with *Michlet*.

Length on waterline	11.537 m
Breadth of one hull on waterline	0.767814 m
Draught	0.254 m
Wetted surface of one hull	8.92256 m ²
Width of boat on waterline	6.28972 m
Block coefficient	0.444444
Volume displacement of boat	2 m ³

Table 2.1: Main dimensions of the catamaran analyzed.

Michlet calculates the following resistance components:

- Skin friction
- Form drag
- Hydrostatic resistance of transom stern
- Wave resistance of transverse wave system
- Wave resistance of diverging wave system
- Interference resistance of transverse waves
- Interference resistance of diverging waves

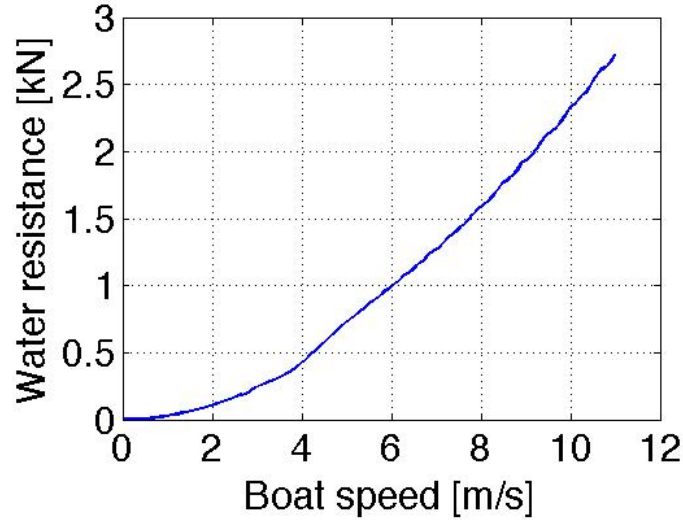


Figure 2.3: Water resistance found with *Michlet*.

The skin friction is calculated using either the ITTC 1957 line

$$C_F = \frac{0.075}{[\log(Re) - 2]^2} \quad (2.1)$$

or Grigson’s algorithm (Grigson, 2000). In Fig. 2.3, the ITTC 1957 line is used. The wave resistance is calculated using Michell’s thinship theory (Michell, 1898), augmented for, among others, transom stern effects and boundary layer displacement thickness. *Michlet* has proven to calculate the resistance of a wide variety of hulls, especially slender hulls, with good accuracy (see the file `mlt806_verification.xls` in the “docs” folder of *Michlet* for details).

2.4 Velocity prediction method

Fig. 2.4 shows a windmill driven catamaran sailing straight upwind. F_W is the backward force, or thrust, on the wind turbine, F is the forward force produced by the underwater propeller, F_D is the water drag force on the boat, and F_{Da} is the air drag force on the boat. The net force ($F - F_W$) produces the forward speed, u , of the boat, at which $F - F_W - F_D - F_{Da} = 0$.

Fig. 2.5 shows the wind and boat velocity vectors for a windmill boat sailing

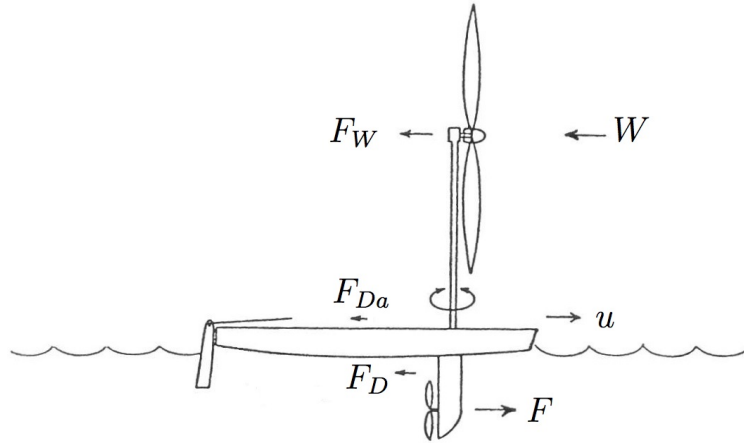


Figure 2.4: Sketch of a windmill boat (catamaran) sailing upwind. Modified from (Blackford, 1985a).

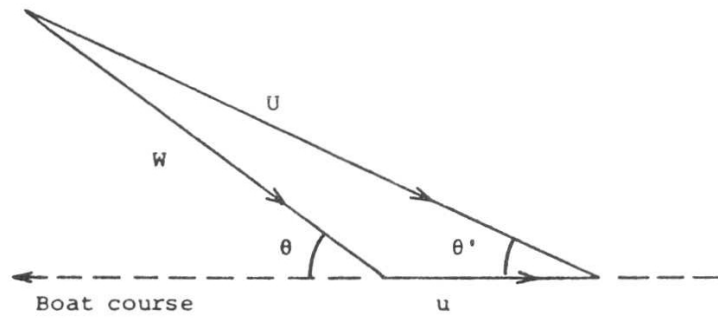


Figure 2.5: Sketch of wind and boat velocity vectors (Blackford, 1985a).

at an angle θ with respect to the true wind. U is the apparent wind speed, which makes an angle θ' with respect to the boat course, W is the wind speed, and u is the speed of the boat.

The iteration process to find the steady-state boat speed is as follows:

1. Choose a boat speed, u , and a wind speed, W .

The apparent wind speed is given as (Blackford, 1985a)

$$U = W(1 + f^2 + 2f \cos \theta)^{1/2} \quad (2.2)$$

where $f = u/W$ is the boat speed to wind speed ratio.

The angle θ' , which is the angle between the apparent wind and the boat course, is given as (Blackford, 1985a)

$$\cos \theta' = \pm \left[1 - \left(\frac{W \sin \theta}{U} \right)^2 \right]^{1/2} \quad (2.3)$$

where the plus sign is to be used for $0 < \theta' < \pi/2$ and the minus sign for $\pi/2 < \theta' < \pi$. When $\theta' > \pi/2$, F_W is actually helping the boat forward.

2. Calculate the wind velocity loss due to the wind turbine, ΔU , from the definition of wind turbine efficiency:

$$\eta_t = \frac{\frac{1}{2}\rho_a Q [U^2 - (U - \Delta U)^2]}{\frac{1}{2}\rho_a U^3 A_t} \quad (2.4)$$

where the volume flow through the wind turbine disk of disk area A_t is given from momentum theory, see Appendix A.1, as

$$Q = A_t \left(U - \frac{\Delta U}{2} \right) \quad (2.5)$$

Equation 2.4 gives us a cubic equation for ΔU which can be solved in e.g. Matlab:

$$\frac{(\Delta U)^3}{2} - 2U(\Delta U)^2 + 2U^2\Delta U - U^3\eta_t = 0 \quad (2.6)$$

Note that Eq. 2.6 has no solution if $\eta_t > 16/27$, see Fig. 2.6. $\eta_t = 16/27$ is known as Betz limit.

3. Calculate the component of the thrust on the wind turbine in the direction of the boat course, from momentum theory, see Appendix A.1, as

$$F_W = \rho_a Q \Delta U \cos \theta \quad (2.7)$$

The component of the thrust on the wind turbine normal to the boat course will give the boat a heel angle, but assuming that this force is balanced, e.g. by a keel, it can be ignored.

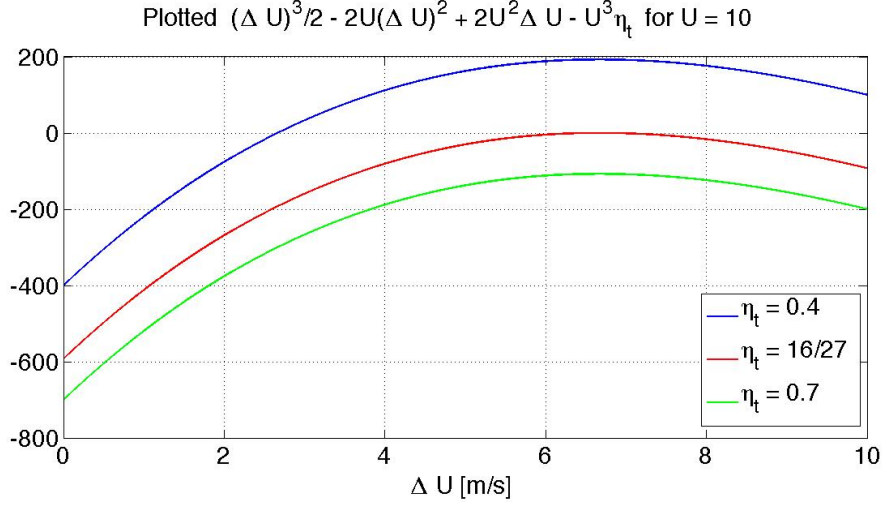


Figure 2.6: Relation between Eq. 2.6 and Betz limit.

4. Calculate the general air resistance as

$$\begin{aligned}
 F_{Da} = & C_{D,boat,air} \frac{1}{2} \rho_a (U \cos \theta')^2 A_{boat,air} \\
 & + C_{D,mast} \frac{1}{2} \rho_a ((U - \Delta U) \cos \theta')^2 A_{mast,covered} \\
 & + C_{D,mast} \frac{1}{2} \rho_a (U \cos \theta')^2 A_{mast,uncovered}
 \end{aligned} \tag{2.8}$$

where $A_{boat,air}$ is the projected frontal area above the waterline of the boat, $A_{mast,covered}$ is the projected area of the part of the mast that is covered by the wind turbine, and $A_{mast,uncovered}$ is the projected area of the part of the mast that is not covered by the wind turbine. It is assumed here that the wind is slowed down to $U - \Delta U$ at the mast. In reality, the wind is slowed down to somewhere between $\frac{\Delta U}{2}$ and ΔU at the mast, as the mast is relatively close to the wind turbine, see Appendix A.1. This method of calculating the air resistance of the boat does not include the effect of lift due to the hull shape. It also assumes a constant C_D for both the projected frontal and the rear area above the waterline of the boat. Values for $C_D \cos \theta'$ can be found in e. g. (Brix, 1993) for different ship types. The error by using the method above however, is small, since the air resistance is small compared to the water resistance.

5. Calculate the total water resistance on the hull with a computer program, e. g. *Michlet*. Enter the resistance curve with the u value and read off the resistance, F_D .

6. Calculate the propeller thrust from the requirement that the power from the wind turbine must equal the power required to propel the boat forward at speed u , if no energy is stored on the boat:

$$\frac{Fu}{\eta_p} = \frac{1}{2}\rho_a U^3 A_t \eta_t \eta_g \quad (2.9)$$

7. Check if $F = F_D + F_{Da} + F_W$. Since F_{Da} is proportional to $\cos^2 \theta'$, F_{Da} will be positive for all θ' . When $\theta' > \frac{\pi}{2}$, F_{Da} will help the boat forward, so then one must check if $F = F_D - F_{Da} + F_W$. F_W is proportional to $\cos \theta'$, so F_W will automatically be negative when $\theta' > \frac{\pi}{2}$.

8. When 7. is true, the boat will move at a constant speed u .

The propeller efficiency, η_p , can be found from open water tests of a given propeller, see Fig. 2.7. The open water characteristics in Fig. 2.7 is valid for a four-bladed propeller with pitch ratio $P/D = 1.042$ and expanded blade area ratio $EAR = A_E/A_p = 0.52$. If the propeller is mounted between the two hulls of a catamaran, the wake fraction and thrust reduction are both minimal, the propeller advance velocity is approximately u , and η_0 from an open water test can be used as propeller efficiency η_p .

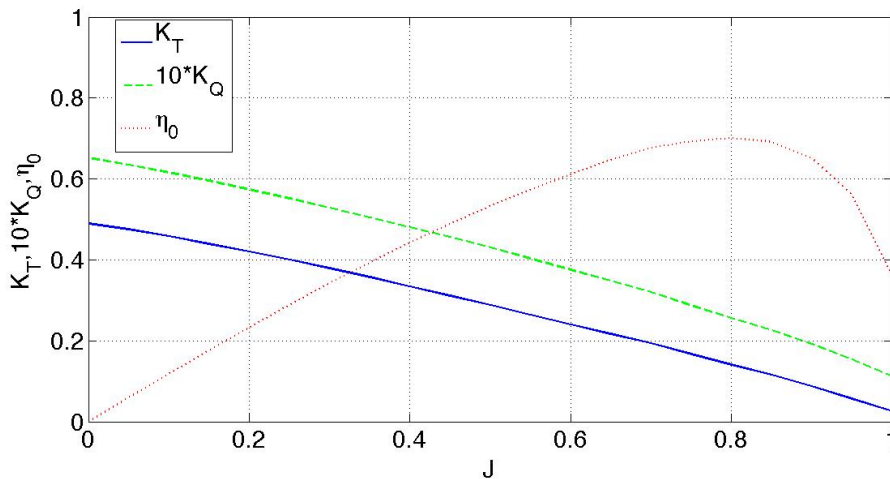


Figure 2.7: Open water diagram.

In order to find η_0 , one must know the advance number, $J = \frac{u}{nD}$, for a given boat speed. The revolution speed, n , can be eliminated by plotting $\frac{K_Q}{J^3}$ vs

J , see Fig. 2.8, where $K_Q = \frac{Q}{\rho_w n^2 D^5}$ is the torque coefficient plotted in the open water diagram. The advance number at a given boat speed can then be found by entering the $\frac{K_Q}{J^3}$ vs J curve with the value

$$\frac{K_Q}{J^3} = \frac{Q}{\rho_w n^2 D^5} \frac{n^3 D^3}{u^3} = \frac{P_D}{\rho_w 2\pi u^3 D^2} \quad (2.10)$$

and read off the corresponding J value. The power from the wind turbine after transmission losses, P_D , equals the power delivered to the propeller:

$$P_D = 2\pi n Q = \frac{1}{2} \rho_a U^3 A_t \eta_t \eta_g \quad (2.11)$$

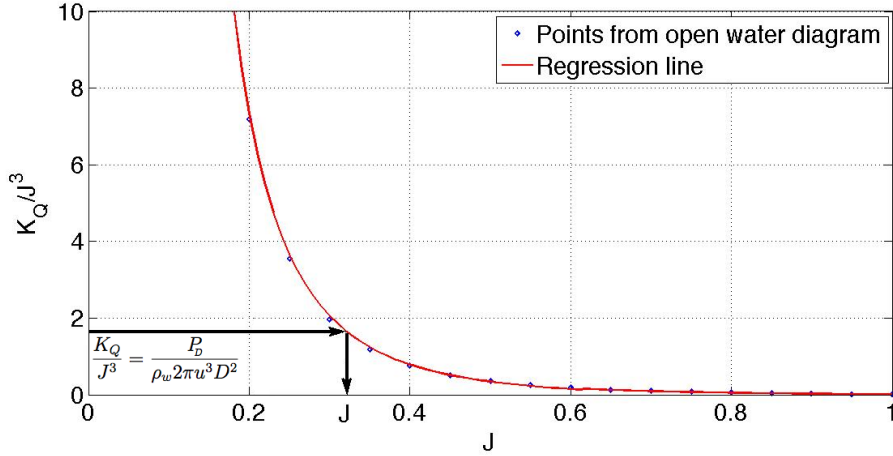


Figure 2.8: K_Q/J^3 vs J .

This can be done numerically by calculating a regression line based on the $\frac{K_Q}{J^3}$ vs J values from the open water diagram. Due to the flatness of this curve for high J values, it is very important that the regression line is accurate, since entering the regression line with a low $\frac{K_Q}{J^3}$ value will give a totally wrong J value, if the regression line is just slightly inaccurate for high J values. We see from Fig. 2.7 that η_0 reaches a peak around $J = 0.8$ and then declines for higher J values, hence the propeller thrust also declines for $J > 0.8$.

The resulting propeller efficiency as a function of the boat speed is shown in Fig. 2.10 for $\theta = 0$. The reason for the small bump in the propeller efficiency around $u = 1.7$ m/s is that the regression curve in Fig. 2.8 consists of two power functions connected at $J = 0.613$, for maximum accuracy of the regression line.

Fig. 2.9 shows the propeller thrust and boat resistance for the 11.5 m long catamaran in 5 m/s wind, directly upwind. $A_{boat,air} = 4 \text{ m}^2$, $A_{mast,covered} = 1.8 \text{ m}^2$, $A_{mast,uncovered} = 0.6 \text{ m}^2$, $C_{D,boat,air} = 0.7$, $C_{D,mast} = 1.17$, $R = 4 \text{ m}$, $D = 0.8 \text{ m}$, $\eta_t = 0.4$, and $\eta_g = 0.90$, are used here. The water propeller used is the same as for the open water diagram, Fig. 2.7. The green dot marks the thrust at zero advance velocity, calculated, see Appendix A.3, as

$$F_0 = (\rho_w \pi \eta_{p0}^2)^{1/3} (D^2 P_D^2)^{1/3} \quad (2.12)$$

where η_{p0} is the propeller efficiency at zero advance velocity.

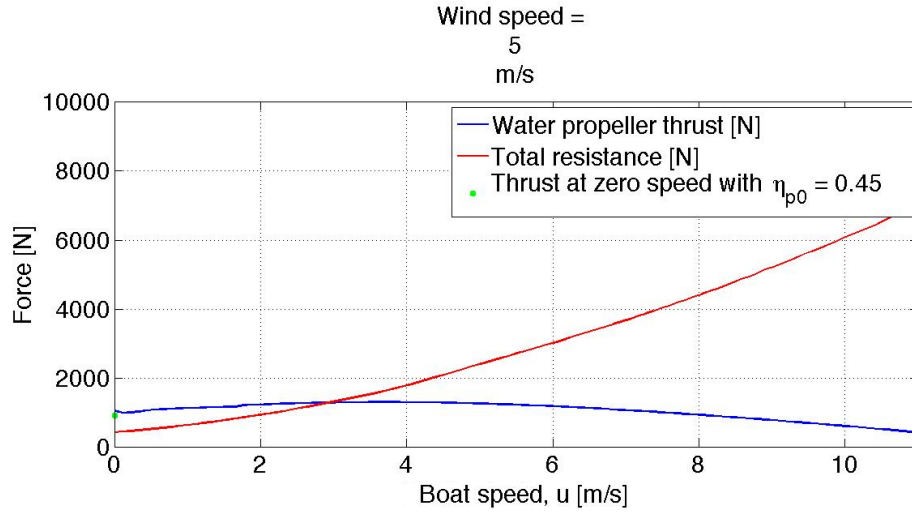


Figure 2.9: Thrust vs resistance, $\theta = 0^\circ$.

Fig. 2.11 shows the effect of the propeller diameter on the boat speed to wind speed ratio, f , for three different wind speeds, sailing upwind. We see that the propeller diameter resulting in the highest f is $D = 0.8 \text{ m}$, for all three wind speeds. $D = 0.8 \text{ m}$ is thus used in all calculations here. In both Fig. 2.10 and Fig. 2.14, it is assumed calm water and a constant wind turbine efficiency of 0.4 for all wind speeds. In reality, the wind turbine efficiency is highly dependent on the wind speed, as we can see from Fig. 5.11. Furthermore, higher wind speeds will generate bigger waves that will give added resistance and lower boat speed to wind speed ratios.

Taking these two aspects into account, the boat speed to wind speed ratio will not be constant with the wind speed, as was also found in experiments by Blackford (Blackford, 1985b) on a full-scale wind turbine boat. The resulting boat speed upwind of about 0.6 times the wind speed is in good agreement

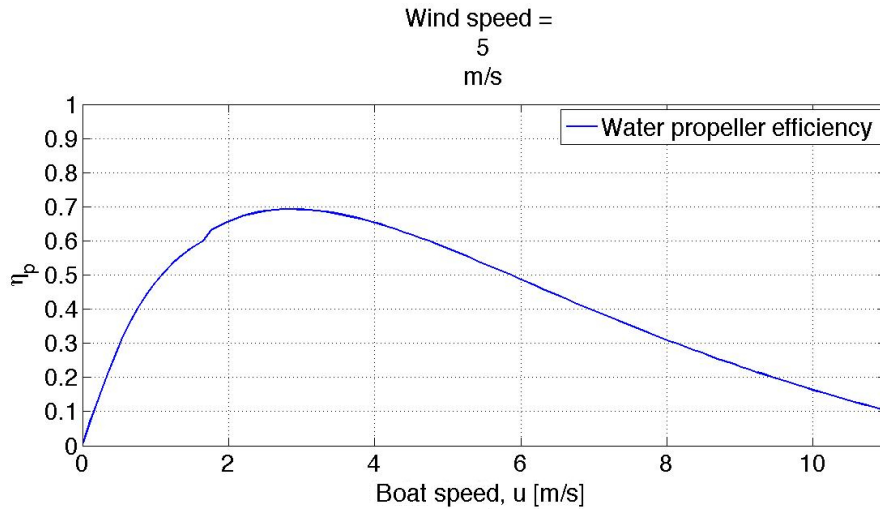


Figure 2.10: Water propeller efficiency, $\theta = 0^\circ$.

with Blackford's experiments on an optimized 4 m wind turbine powered catamaran (Blackford, 1985b), having a four-bladed wind turbine of blade radius 1.90 m. Blackford achieved boat speed to wind speed ratios declining with the wind speed as $f = 0.60 - 0.021W$ sailing upwind, for wind speeds in the range $3 < W < 8$ m/s. There is, however, little agreement with Bose and Wilkinson's results of the testing of the less optimal 8 m catamaran *Revelation*, which was equipped with a 6.10 m diameter wind turbine Bose and Wilkinson (1985). *Revelation* reached on average a boat speed to wind speed ratio of $f = 0.34$ upwind, which decreased to $f = 0.26$ downwind. Also in this case, it was observed that the boat speed to wind speed ratios decreased with increasing wind speed.

Figure 2.12 shows the thrust vs resistance graphs for $\theta = 90^\circ$, for the same boat characteristics as above. The wind speed is 5 m/s.

Figure 2.13 shows the thrust vs resistance graphs directly downwind, $\theta = 180^\circ$, for the same boat characteristics as above. The wind speed is 5 m/s.

Fig. 2.14 shows boat speed to wind speed ratios, f , for all wind angles, for three different wind speeds. Assuming calm water and constant wind turbine efficiency for all three wind speeds, we see that the boat speed to wind speed ratios are approximately equal for all wind speeds. The reason for the discrete values in Fig. 2.14 and Fig. 2.11 is that the hull resistance is calculated for a discrete number of boat speeds with *Michlet*.

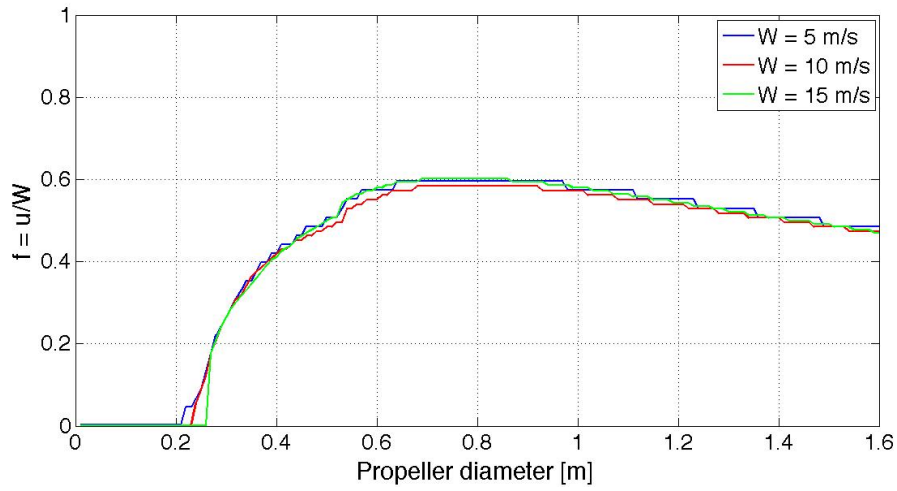


Figure 2.11: Water propeller diameter vs f , $\theta = 0^\circ$.

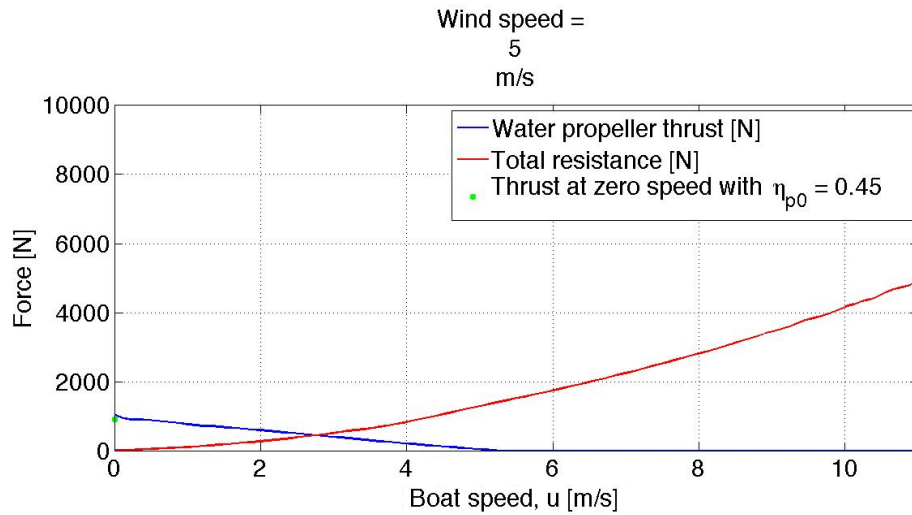


Figure 2.12: Thrust vs resistance, $\theta = 90^\circ$.

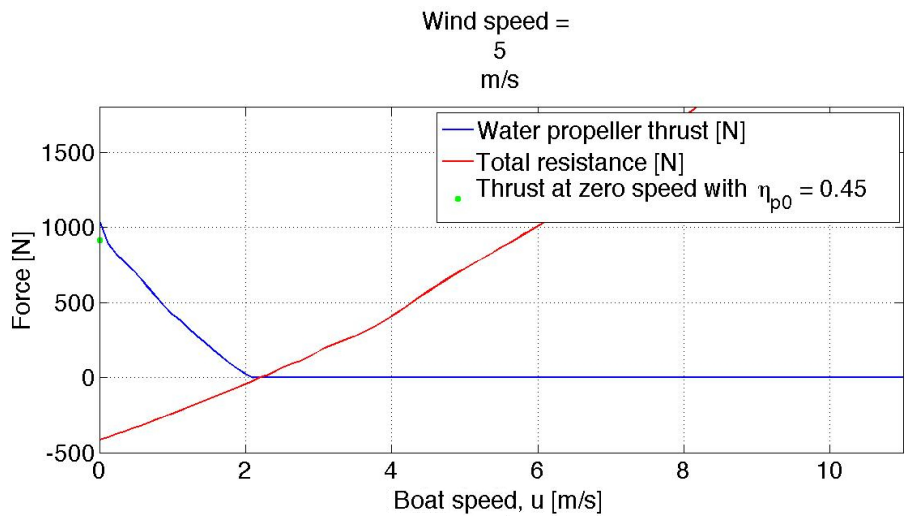


Figure 2.13: Thrust vs resistance, $\theta = 180^\circ$.

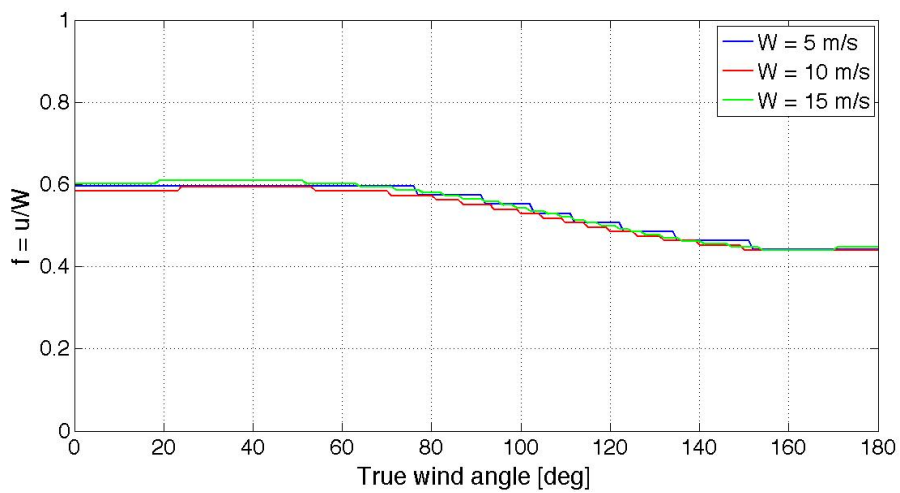


Figure 2.14: Boat speed to wind speed ratio vs true wind angle.

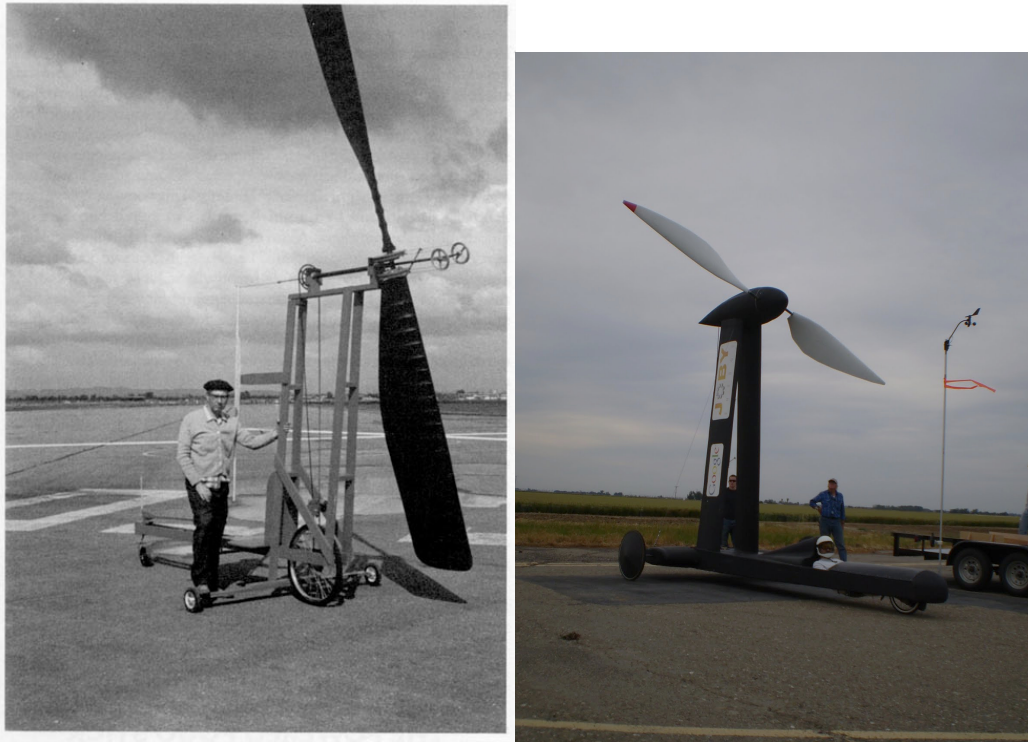
3 Directly Downwind Faster Than The Wind?

3.1 Introduction

A related topic to wind turbine propulsion is the reversed configuration, where, instead of a wind turbine driving a water propeller, a water turbine is driving an air propeller. The interesting feature of this configuration is its unique theoretical ability to propel a boat faster than the wind, directly downwind. This configuration is much less studied in the literature than wind turbine propulsion, but in light of recent academic interest (Drela, 2009a,b), and due to the fact that a turbine and a propeller are two sides of the same coin, the present section is included here. Another reason for including the present section, is that the momentum theory approach of Sec. 2.4 is suitable for studying the performance of a vessel employing this configuration, sailing downwind at wind speed and faster. The configuration where a water turbine is driving an air propeller can only be used sailing downwind, where the wind provides the necessary push on the air propeller to get the water vehicle moving. Sailing downwind at other wind directions than directly downwind, using this configuration, has not been studied here, since momentum theory can only be used when the propeller disk is perpendicular to the incoming flow.

The question of whether it is possible to move Directly Downwind Faster Than The Wind (DDFTTW) on a level surface, powered by wind energy only, was answered by Andrew Bauer in 1969. In (Bauer, 1969) he describes the theoretical performance of land and water vehicles, designed to go DDFTTW. Bauer also constructed such a land vehicle, and test results showed that his vehicle did in fact go Directly Downwind Faster Than The Wind, going approximately 1.17 times faster than the wind speed in a 5.4 m/s wind.

As far as the author is aware of, no DDFTTW water vehicles have been built. In 2010, Bauer's experiment was recreated by a team of students along with their professor and advisors at San Jose State University (SJSU) (Borton et al., 2010), who successfully built a man-carrying wind powered land vehicle which reached a speed of almost three times the wind speed, sailing directly downwind (Barry, 2010; Discovery Channel, 2010). At the time of writing, a record run with official verification by the North American Land Sailing Association (NALSA) is in the plans.



(a) Dr. Bauer and his vehicle (Borton et al., 2010), (b) The SJSU vehicle of 2010 (Borton et al., 2010)

Figure 3.1: The original and a modern full-scale DDFTTW cart.

In order for a boat to sail faster than the wind, directly downwind, powered by only the wind itself, the configuration with water propeller and wind turbine must be reversed, so that the water propeller is now a water turbine and the wind turbine is now an air propeller. Fig. 3.2 shows the wind and velocity vectors when the boat is moving directly downwind, faster than the wind. Is it possible to reach $u > W$ using this configuration? This is discussed in Sec. 3.4.

3.2 Velocity prediction

Fig. 3.3 illustrates the flow through the air propeller disk for a range of propeller conditions. The ring vortex state occurs when the boat is driven downwind by the air propeller, but not faster than the wind speed, W . Bauer compared experimental data by Glauert (Glauert, 1943) for the propeller

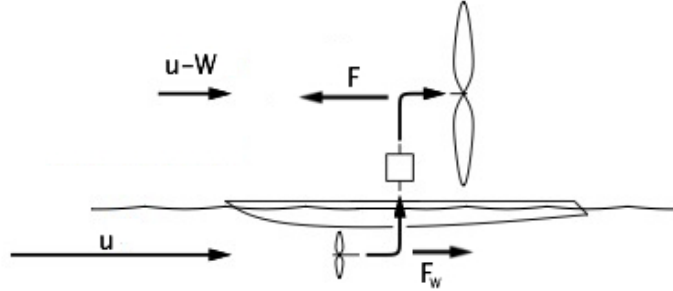


Figure 3.2: Apparent velocities, DDFTTW. Modified from (Drela, 2009a).

thrust in the ring vortex state with the propeller thrust predicted using momentum theory, and chose due to meagerness of the experimental data and a fair correspondence between the experimental data and momentum theory to use momentum theory in his calculations of the thrust in the ring vortex state. In Sec. 3.4, the propeller force in still air is studied, and according to Glauert, momentum theory can be used in this propeller state. The expression for the inviscid part of the propeller efficiency, Eq. 3.8, is derived from momentum theory, and using this to find the propeller thrust, as in Eq. 3.10, implies that momentum theory is used here to find the propeller thrust when the propeller is operating in still air.

The iteration process to find the steady-state boat speed, assuming that the boat is capable of sailing downwind faster than then wind, is similar to the procedure in Sec. 2.4:

1. Choose a wind speed, W , and a boat speed, u , that is higher than W .
2. Calculate the water velocity loss due to the water turbine, Δu , from the following definition of water turbine efficiency:

$$\eta_{t,w} = \frac{\frac{1}{2}\rho_w Q [u^2 - (u - \Delta u)^2]}{\frac{1}{2}\rho_w u^3 A_{t,w}} \quad (3.1)$$

where the volume flow through the water turbine disk of disk area $A_{t,w}$ is given from momentum theory as

$$Q = A_{t,w} \left(u - \frac{\Delta u}{2} \right) \quad (3.2)$$

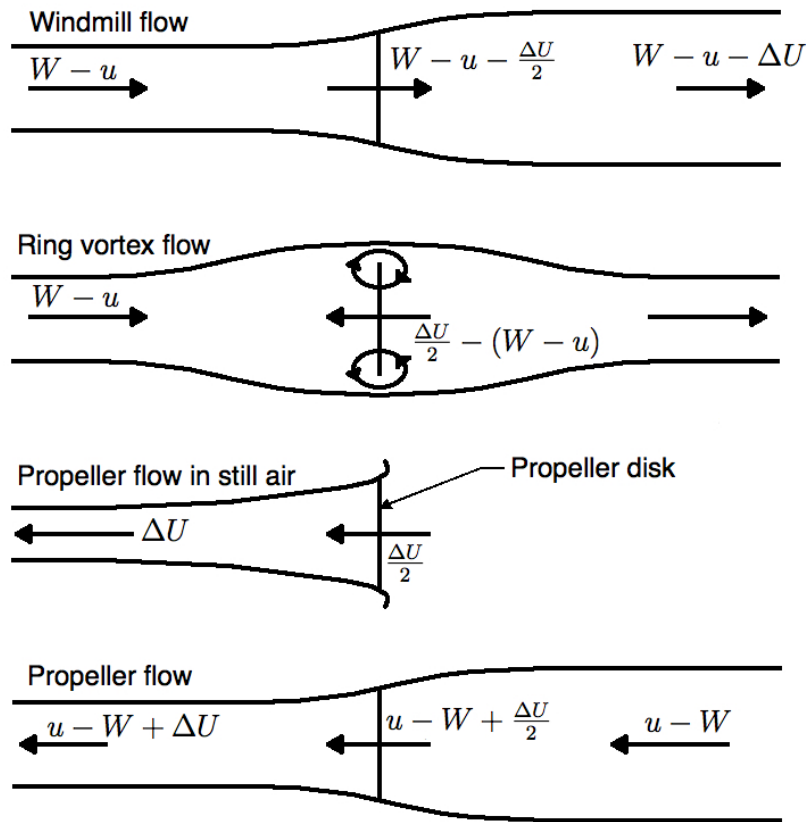


Figure 3.3: Different flow regimes of a propeller. Modified from (Bauer, 1969).

Equation 3.1 gives us a cubic equation for Δu which can be solved in e.g. Matlab:

$$\frac{(\Delta u)^3}{2} - 2u(\Delta u)^2 + 2u^2\Delta u - u^3\eta_{t,w} = 0 \quad (3.3)$$

3. Calculate the thrust on the water turbine from momentum theory as

$$F_W = \rho_w Q \Delta u \quad (3.4)$$

4. Calculate the general air resistance as

$$F_{Da} = C_{D,boat,air} \frac{1}{2} \rho_a (u - W)^2 A_{boat,air} + C_{D,mast} \frac{1}{2} \rho_a (u - W)^2 A_{mast} \quad (3.5)$$

if the mast is now upwind of the propeller.

5. Calculate the total water resistance on the hull with a computer program, e. g. *Michlet*. Enter the resistance curve with the u value and read off the resistance, F_D .

6. Calculate the air propeller thrust from

$$\frac{F(u - W)}{\eta_{p,a}} = \frac{1}{2} \rho_w u^3 A_{t,w} \eta_{t,w} \eta_g \quad (3.6)$$

where $\eta_{p,a}$ is the air propeller efficiency, $A_{t,w}$ is the water turbine disk area, and $\eta_{t,w}$ is the water turbine efficiency, defined in Eq. 3.1.

7. Check if $F = F_W + F_{Da} + F_D$

8. When 7. is true, the boat will move at a constant speed u .

3.3 Propeller efficiency

With a fixed $\eta_{p,a}$, the propeller thrust F in Eq. 3.6 approaches infinity as u approaches W . To avoid this, a clever expression for $\eta_{p,a}$ is used, adopted from (Drela, 2009a). The air propeller efficiency can be broken down into a viscous efficiency, $\eta_{v,a}$, and an inviscid efficiency, $\eta_{i,a}$, taken from momentum theory, see Appendix A.2. $\eta_{i,a}$ is modified by including a swirl efficiency, $\eta_{swirl,a}$, to account for non-axial velocities in the propeller slipstream.

$$\eta_{p,a} = \eta_{i,a} \eta_{v,a} \quad (3.7)$$

$$\eta_{i,a} = \frac{2}{1 + \sqrt{1 + \frac{2F}{\rho_a (u - W)^2 A_{p,a} \eta_{swirl,a}}}} \quad (3.8)$$

Inserting equation 3.8 into equation 3.6 yields

$$\frac{F(u - W)}{2\eta_{v,a}} \left[1 + \sqrt{1 + \frac{2F}{\rho_a(u - W)^2 A_{p,a} \eta_{swirl,a}}} \right] = \frac{1}{2} \rho_w u^3 A_{t,w} \eta_{t,w} \eta_g \quad (3.9)$$

$$\Rightarrow F + F \sqrt{1 + \frac{2F}{\rho_a(u - W)^2 A_{p,a} \eta_{swirl,a}}} = \frac{\rho_w u^3 A_{t,w} \eta_{t,w} \eta_g \eta_{v,a}}{u - W} \quad (3.10)$$

This can be written as

$$F + F \sqrt{1 + aF} = b \quad (3.11)$$

where

$$a = \frac{2}{\rho_a(u - W)^2 A_{p,a} \eta_{swirl,a}} \quad (3.12)$$

and

$$b = \frac{\rho_w u^3 A_{t,w} \eta_{t,w} \eta_g \eta_{v,a}}{u - W} \quad (3.13)$$

which results in the cubic equation

$$aF^3 + 2bF - b^2 = 0 \quad (3.14)$$

Equation 3.14 can then be solved numerically in e.g. Matlab to find F . As is shown in Sec. 3.4, this expression for F will have a final value when u approaches W .

3.4 Overcoming drag at the wind speed

To overcome the water and air resistance of the boat,

$$F_{net} = F - F_W \geq F_{Da} + F_D \quad (3.15)$$

The water resistance of a hydrofoil boat is approximately proportional to the boat speed squared, when the hydrofoil boat is “flying”. When the boat is sailing downwind at wind speed, $F_{Da} = 0$. As is proven below, the

force available to overcome the boat resistance at $u = W$, $F_{net,@u=W}$, is also proportional to u^2 .

Since both the boat resistance and the force available to overcome the boat resistance are proportional to u^2 for all values of $u = W$, the factor that determines if the boat will go DDFTTW is the ratio a_2/a_1 , where the boat resistance is

$$F_D = a_1 u^2 \quad (3.16)$$

and F_{net} at $u = W$ is

$$F_{net,@u=W} = a_2 u^2 \quad (3.17)$$

In other words, the boat will go DDFTTW if $a_2 > a_1$.

The boat resistance can be obtained from towing tests or computed using a hull resistance program, and a_1 can be calculated as

$$F_D = \frac{1}{2} \rho_w S u^2 C_T \quad (3.18)$$

$$a_1 = \frac{1}{2} \rho_w S C_T \quad (3.19)$$

where S is the wetted surface of the boat and C_T is the total resistance coefficient.

Finding a_2 is a more complicated affair. In order to prove that F_{net} is proportional to u^2 when $u = W$, let us first look at F_W . The thrust on the water turbine is given by Eq. 3.4. The loss of water velocity at the turbine disc can be calculated from another definition of the water turbine efficiency, namely the ideal efficiency of a water turbine using the inverse propeller efficiency definition:

$$\eta_{t,w,2} = \frac{P}{F_W u} \quad (3.20)$$

where P is the power from the water turbine, found as $\frac{1}{2} \rho_w Q [u^2 - (u - \Delta u)^2]$ in Eq. 3.1. Combining Eq. 3.20, Eq. 3.1, Eq. 3.2, and Eq. 3.4, we then get

$$\eta_{t,w,2} = 1 - \frac{\frac{1}{2} \Delta u}{u} \quad (3.21)$$

$$\Rightarrow \Delta u = 2u(1 - \eta_{t,w,2}) \quad (3.22)$$

Inserting Eq. 3.22 into Eq. 3.4 yields

$$F_W = 2\rho_w A_{t,w} \eta_{t,w,2} (1 - \eta_{t,w,2}) u^2 \quad (3.23)$$

from which we can see that F_W is proportional to u^2 , assuming that $\eta_{t,w,2}$ is constant with the boat speed u .

To prove that also F is proportional to u^2 at $u = W$, and hence that $F_{net} = F - F_W$ is proportional to u^2 at $u = W$, let us start with Eq. 3.10 and take the limit as u approaches W . If we square Eq. 3.10 and denote

$$c = \frac{2}{\rho_a A_{p,a} \eta_{swirl,a}} \quad (3.24)$$

and

$$d = \rho_w u^3 A_{t,w} \eta_{t,w} \eta_g \eta_{v,a} \quad (3.25)$$

we get

$$2F^2 \left(1 + \sqrt{1 + \frac{cF}{(u-W)^2}} \right) + \frac{cF^3}{(u-W)^2} = \frac{d^2}{(u-W)^2} \quad (3.26)$$

As u approaches W , the expression under the root is approximately $\frac{cF}{(u-W)^2}$, and due to the root, the first term of Eq. 3.26 will be approximately proportional to $\frac{1}{u-W}$. Hence, as u approaches W , the other two terms in Eq. 3.26 will dominate and will be the two terms that we are left with. We are then left with

$$\frac{cF^3}{(u-W)^2} = \frac{d^2}{(u-W)^2} \quad (3.27)$$

$$\Rightarrow F = \left(\frac{d^2}{c} \right)^{1/3} = \left(\frac{(\rho_w u^3 A_{t,w} \eta_{t,w} \eta_g \eta_{v,a})^2}{\frac{2}{\rho_a A_{p,a} \eta_{swirl,a}}} \right)^{1/3} \quad (3.28)$$

$$F = \left(\frac{\rho_a A_{p,a} \eta_{swirl,a}}{2} \right)^{1/3} (\rho_w A_{t,w} \eta_{t,w} \eta_g \eta_{v,a})^{2/3} u^2 \quad (3.29)$$

and we see that F at $u = W$ is proportional to u^2 , and hence that also F_{net} at $u = W$ is proportional to u^2 , assuming that $\eta_{t,w}$ is constant with the boat speed u .

Finally, a_2 is found as

$$a_2 = \left(\frac{\rho_a A_{p,a} \eta_{swirl,a}}{2} \right)^{1/3} (\rho_w A_{t,w} \eta_{t,w} \eta_g \eta_{v,a})^{2/3} - 2\rho_w A_{t,w} \eta_{t,w,2} (1 - \eta_{t,w,2}) \quad (3.30)$$

where the relationship between the two definitions of the water turbine efficiency is

$$\eta_{t,w} = \frac{2(u - \frac{\Delta u}{2})\Delta u \eta_{t,w,2}}{u^2} \quad (3.31)$$

3.5 Designing the boat to go DDFTTW

In order for the boat to go DDFTTW, obviously a_1 should be as small as possible, and a_2 as large as possible. A hydrofoil boat will have significantly less water resistance than a displacement hull once the hydrofoil boat is “flying”. What limits the value of a_1 is the size of the hydrofoil boat, which must be large enough to balance the moment due to the air propeller as well as providing enough lift to lift the hull out of the water. With ρ_a , $\eta_{swirl,a}$, ρ_w , η_g and $\eta_{v,a}$ being constants, the parameters that can be adjusted in order to maximize a_2 are $A_{p,a}$, $A_{t,w}$ and $\eta_{t,w}$.

With an air propeller diameter of 6 m, $\eta_g = 0.90$, $\eta_{v,a} = 0.90$, and $\eta_{swirl,a} = 0.95$, Fig. 3.4 shows a_2 as a function of water turbine diameter and $\eta_{t,w}$. According to Drela (Drela, 2009a), these values of η_g , $\eta_{v,a}$, and $\eta_{swirl,a}$ are conservative.

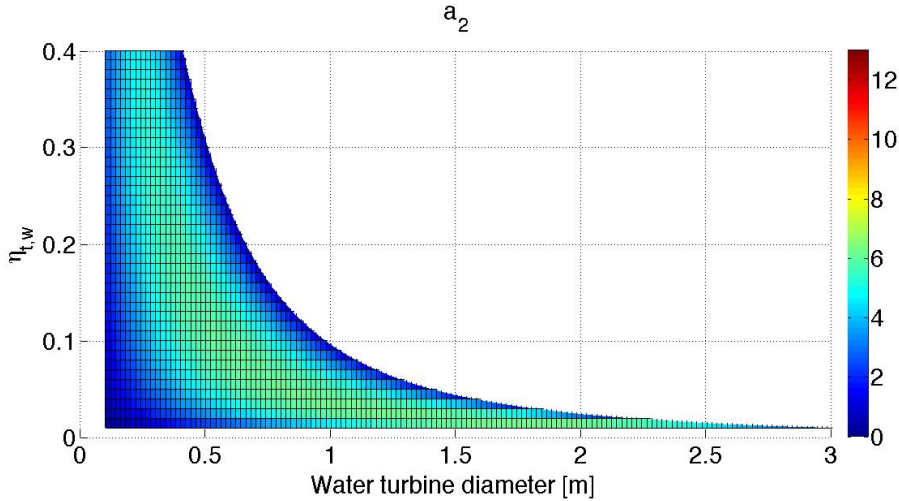


Figure 3.4: a_2 as a function of water turbine diameter and $\eta_{t,w}$.

In order to maximize a_2 , a very low $\eta_{t,w}$ and a fairly large water turbine diameter should be chosen. $\eta_{t,w}$ can be reduced by reducing the solidity ratio of the water turbine rotor and adjusting the blade pitch angle. The resulting optimal water turbine will thus have long thin blades and bear more resemblance to an airplane propeller than a boat propeller.

As we see from Fig. 3.4, the maximum value of a_2 is around 6. For the boat to go DDFTTW, this means that $a_1 = \frac{1}{2}\rho_w SC_T < 6$. Reaching $a_1 < 6$ is difficult due to design limitations. For hydrofoils, the equivalent of SC_T in the expression for a_1 , Eq. 3.19, is $SC_T = A_p C_D$, where A_p is the projected area of the hydrofoil in the direction of the lift (close to the chord length times the span for one hydrofoil), and C_D is the hydrofoil drag coefficient, which is with respect to A_p .

The relation between the three-dimensional lift coefficient, C_L , and the sectional lift coefficient, c_l , found in (Abbott and von Doenhoff, 1959) for a specific foil section, is for an elliptical circulation distribution

$$C_L = \frac{c_l}{1 + \frac{2}{Asp}} \quad (3.32)$$

where Asp is the aspect ratio of the hydrofoil.

C_D is given from Eq. 3.34, where the induced drag coefficient is

$$C_{Di} = \frac{C_L^2}{\pi Asp} \quad (3.33)$$

with elliptical circulation distribution, which is the circulation distribution which gives the least induced drag. The viscous drag coefficient, C_{Dv} can be found in (Abbott and von Doenhoff, 1959) for a specific foil section, where it is denoted c_d .

$$C_D = C_{Di} + C_{Dv} \quad (3.34)$$

For a smooth NACA 0009 foil section, at $Re = 3e6$, the sectional drag coefficient is $c_d = 0.008$ when the sectional lift coefficient is $c_l = 0.7$. Assuming that the boat weighs 2000 kg, that four hydrofoils shall lift the boat (two on each hull), and that the span of each hydrofoil is $s = 1m$, the required chord length can be determined for each boat speed through an iteration process:

First, an estimate of the required chord length, c' , is calculated using the

sectional lift coefficient, c_l :

$$c' = \frac{L}{\frac{1}{2}\rho_w u^2 c_l 4s} \quad (3.35)$$

where $L = mg$, where m is the boat mass, is the required lift.

An estimate of the lift coefficient, C'_L , is calculated using c' to calculate the aspect ratio in Eq. 3.32. Then, an estimate of the lift, L' , is calculated using C'_L and c' :

$$L' = \frac{1}{2}\rho_w u^2 C'_L 4sc' \quad (3.36)$$

Finally, c' is corrected from the relation

$$c = c' \frac{L}{L'} \quad (3.37)$$

which converges to the correct c as L' approaches L when the iteration procedure is repeated, now using L' in Eq. 3.35

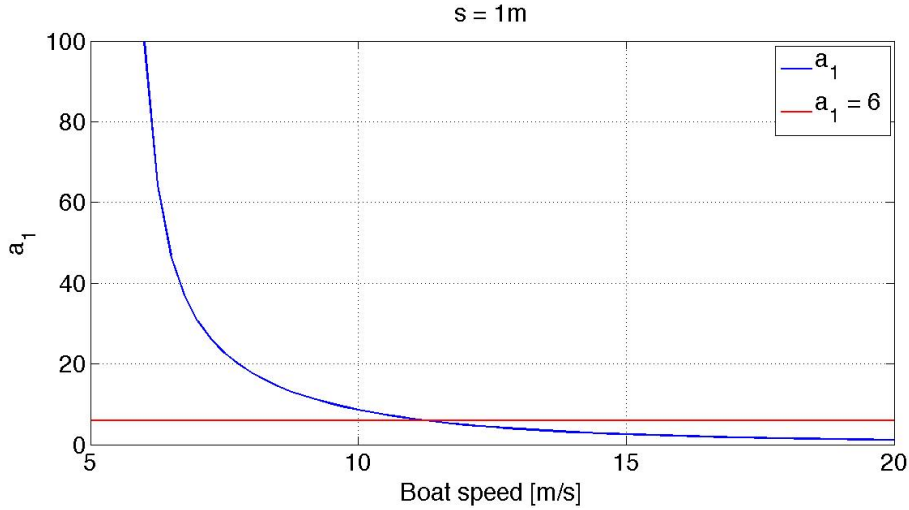


Figure 3.5: a_1 for a hydrofoil boat.

The contribution to a_1 from the struts can be calculated using the empirical formulas given in (Minsaas and Steen, 2008), assuming that the struts are as long as the chord length, the maximum thickness of the struts are 0.2 times the chord length, there are two struts on each hull, and the underwater height

Boat speed [m/s]	a_1 [-]	c [m]
5	26820.98	29.201
7.5	22.68	0.473
10	8.58	0.188
12.5	4.35	0.106
15	2.55	0.069
17.5	1.66	0.049
20	1.16	0.0367

Table 3.1: Chord length of hydrofoil for a DDFTTW boat.

of the struts are 0.2 m. Fig. 3.5 shows a_1 , when the drag due to the struts are included, for a hydrofoil boat having four hydrofoils of span $s = 1$ m. The chord length, c , is given in Table 3.1 for some boat speeds. We see that in order for a_1 to be less than 6, the boat must sail faster than 11.25 m/s and have hydrofoils of chord length 0.14 m. The maximum thickness of such a hydrofoil will be only 1.24 cm, which may cause strength problems. Since we are considering a boat sailing at wind speed, this wind speed will cause waves which will give added resistance. Furthermore, in order to construct a hydrofoil boat that is capable of reaching the “flying” condition at a relatively low speed, and stay “flying” when the boat approaches the wind speed, the lift should be controlled by flaps on the hydrofoils, which in turn will increase the resistance.

It is shown here that it is in theory possible to sail faster than the wind, directly downwind, also for a wind powered water vehicle, but practical aspects such as size, weight, and material strength, as well as accelerating while attaining the desired lift with a hydrofoil boat, makes it in practice quite difficult.

4 Optimization of the wind turbine powered boat

4.1 Blade element theory

Brad Blackford showed in (Blackford, 1985a) how to use classical blade element theory to design optimal wind turbine blades for a wind turbine driven boat. Blackford's approach is presented here with the original notation, and applied to show how the optimal blade design for a given wind turbine boat changes for different wind directions.

For an illustration of the wind turbine boat with force and wind vectors, see Fig. 2.4. The wind and velocity vectors of the moving wind turbine boat are illustrated in Fig. 2.5. The apparent wind speed experienced by the rotating blade element at radius r , see Fig. 4.1, is given as

$$V = ([U(1 - a)]^2 + [(1 + a')\Omega r]^2)^{1/2} \quad (4.1)$$

where a is the fractional decrease in wind speed when the wind reaches the blade, a' accounts for the induced rotation of the wind field at the blade, and Ω is the turbine rotation rate in rad/s.

The power extracted from the wind by the blade element of length dr is given as the product of the tangential component of the aerodynamic force acting on the blade element times the tangential velocity component of the blade element, Ωr , i.e.

$$dP = \frac{1}{2}\rho_a c N V^2 (C_L \sin \phi - C_D \cos \phi) \Omega r dr \quad (4.2)$$

where N is the number of blades, ϕ the apparent wind angle, c the chord, and C_L and C_D are the lift and drag coefficients of the blade element respectively.

The forward force produced by the water propeller can be derived from the windmill power as

$$dF = \zeta dP/u \quad (4.3)$$

where ζ is the overall efficiency factor of the driving mechanism, which consists of the shafts, gears, bearings and underwater propeller.

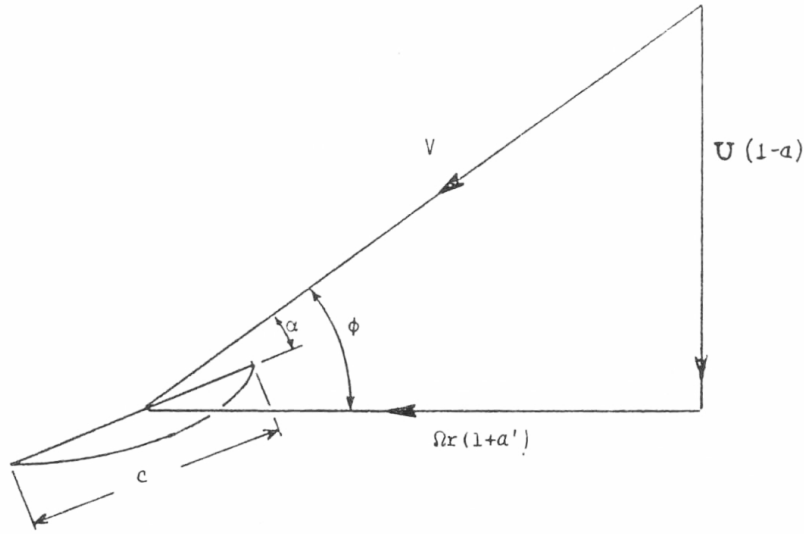


Figure 4.1: Wind turbine blade element with air velocity components (Blackford, 1985a).

The backward force on the wind turbine, due to extraction of power from the wind, will have a component transverse to the motion of the boat as well as parallel to it. Assuming that the transverse force is balanced by a lifting force from the keel, the transverse force component can be ignored. The longitudinal component is given as

$$dF_W = \frac{1}{2} \rho_a c N V^2 (C_L \cos \phi + C_D \sin \phi) dr \cos \theta' \quad (4.4)$$

The net forward force, $dF - dF_W$, is found when combining Eq. 4.2, Eq. 4.3 and Eq. 4.4 as

$$dF - dF_W = \frac{1}{2} \rho_a c C_L N V^2 \left[\zeta \frac{\Omega r}{u} (\sin \phi - \epsilon \cos \phi) - (\cos \phi + \epsilon \sin \phi) \cos \theta' \right] dr \quad (4.5)$$

where $\epsilon = C_D/C_L$ is the drag-to-lift ratio of the airfoil section. From momentum theory, see Appendix A.1, we know that the backward force on the windmill can be written as

$$dF_W = 4 \rho_a U^2 a (1 - a) \pi r dr \cos \theta' \quad (4.6)$$

The power, dP , can be written as

$$dP = \Omega dQ = \frac{1}{2} \rho_a c N V^2 C_L (\sin \phi - \epsilon \cos \phi) \Omega r dr \quad (4.7)$$

where the torque, dQ , exerted on the blade elements by the fluid annulus of thickness dr can from momentum theory, see Appendix A.1, be written as

$$dQ = U(1 - a)4\pi a' \Omega r^3 \rho_a dr \quad (4.8)$$

The alternative expression for dP , $dP = \Omega dQ$, then becomes

$$dP = U(1 - a)4\pi a' \Omega^2 r^3 \rho_a dr \quad (4.9)$$

Combining Eq. 4.9, Eq. 4.3, and Eq. 4.6, the total net forward force can be written as

$$\frac{F_{NET}}{4\pi\rho_a R^2 W^2} = \frac{1 + f^2 + 2f \cos \theta}{S^2} \int_0^S a(1 - a)H(s)s ds \quad (4.10)$$

where R is the wind turbine tip radius, the tip speed ratio is defined as

$$S = \Omega R / U \quad (4.11)$$

the dimensionless speed ratio is defined as

$$s = \Omega r / U \quad (4.12)$$

and the function $H(s)$ is given as

$$H(s) = \zeta \frac{U}{u} \left(\frac{a' s^2}{a} \right) - \cos \theta' \quad (4.13)$$

where U/u can be obtained from Eq. 2.2 and $\cos \theta'$ from Eq. 2.3.

We see from Eq. 4.10 that the overall efficiency factor, ζ , must be large in order to obtain a high boat speed relative to the wind speed, f . We can also see from Eq. 4.5 that small values of the drag-to-lift ratio, ϵ , gives a higher F_{NET} , and thus a higher f .

Now, let us keep ζ , f , and ϵ fixed, set $\theta = 0$, and try to maximize F_{NET} with respect to $a(s)$ and S . Fortunately, a' is related to a , see Appendix A.1, through

$$a'(s) = -\frac{1}{2}(1 + \epsilon/s) + \frac{1}{2}\sqrt{(1 + \epsilon/s)^2 + 4a[(1 - a)/s^2 - \epsilon/s]} \quad (4.14)$$

Blackford could not find an exact analytical function for the $a(s)$ that gives maximum values of F_{NET} . Instead, he found that the function

$$a(s) \simeq a_0[1 - \exp(-2s)] \quad (4.15)$$

gives a good approximation for the maximum F_{NET} values. Indeed, we see from Fig. 4.3 that Eq. 4.15 approximates the maximum $F_{NET}/(4\pi\rho_a R^2 W^2)$ values within about 10% accuracy for tip speed ratios, S , greater than about $S = 0.4$. The exact optimal $a(s)$ in Fig. 4.3 is found by varying $a(s)$ and see which values of $a(s)$ that give the highest F_{NET} values, for all values of s .

In Fig. 4.2 and Fig. 4.3, $\epsilon = 0.03$, $f = 0.5$, and $\zeta = 0.85$. $a_0 = 0.21$ is the value of a_0 that gives the highest values of F_{NET} for all values of s . The optimal value of a_0 depends upon ϵ , f , ζ and θ , as shown in detail in (Blackford, 1985a).

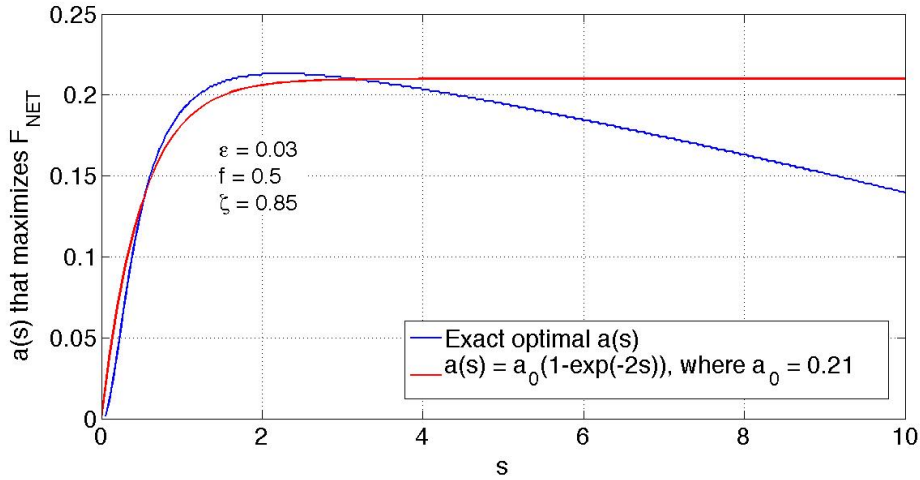


Figure 4.2: The value of $a(s)$ that maximizes F_{net} .

4.2 Optimal apparent wind angle distribution

The optimal apparent wind angle with respect to the blade element, ϕ , can be determined based on the theory described in Sec. 4.1. First, we must assume the boat speed and the wind speed, e. g. $u = 5$ m/s and $W = 10$ m/s. If the boat is sailing upwind, we know from Fig. 4.3 that the maximum F_{NET} is 0.1321, occurring for tip speed ratio $S = 3.5$, with $a_0 = 0.21$, $\epsilon = 0.03$,

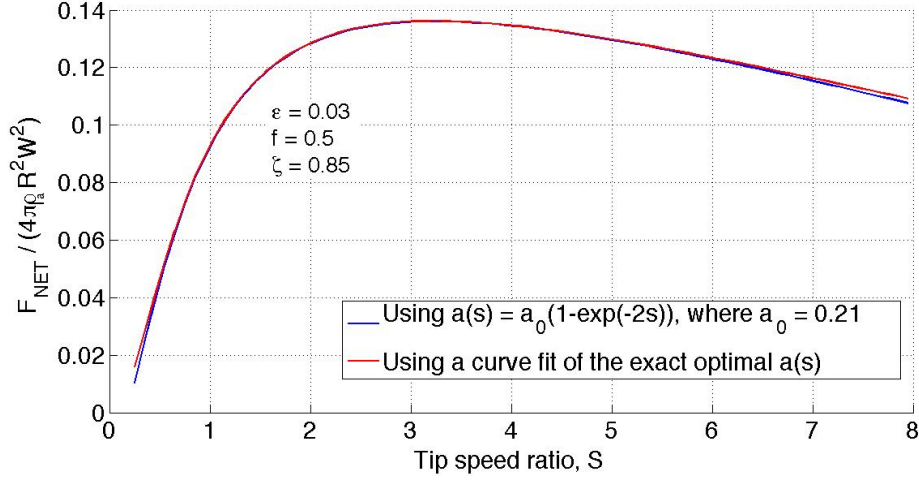


Figure 4.3: Influence of choice of $a(s)$ on the dimensionless net force.

$f = 0.5$, and $\zeta = 0.85$. Assuming that the required net force to propel the boat forward at this boat speed is $F_{NET} = 2000$ N, we can find the wind turbine radius from

$$\frac{F_{NET}}{4\pi\rho_a R^2 W^2} = 0.1321 \quad (4.16)$$

$$\Rightarrow R = \sqrt{\frac{F_{NET}}{4\pi\rho_a W^2 0.1321}} = 3.17m \quad (4.17)$$

using $\rho_a = 1.2$ kg/m³

The apparent wind angle, ϕ , can be found from

$$\phi(s) = \arctan \left[\frac{1}{s} \left(\frac{1-a}{1+a'} \right) \right] \quad (4.18)$$

where a and a' are determined from Eq. 4.15 and Eq. 4.14 respectively. $\phi(r)$ can be found by substituting $s = \frac{\Omega r}{U}$ into Eq. 4.18.

The rotation rate, Ω , is given by

$$\Omega = \frac{SU}{R} \quad (4.19)$$

which gives $\Omega = 16.6$ rad/s under the assumed conditions.

If we design the blades on the basis of giving the boat optimal performance when sailing upwind, R is determined from the required force to propel the

boat upwind. Hence, R will have another value if it is determined from the required force to propel the boat under another wind angle. Blackford found that

$$a_0(\theta) \simeq 0.21 + 0.24(\theta/180)^2 \quad (4.20)$$

is a good approximation for the optimal value of a_0 for different true wind angles, θ . For the optimal tip speed ratio, S , at different true wind angles, θ , Blackford found that

$$S(\theta) \simeq 4 + \theta/90 \quad (4.21)$$

is a good approximation.

Using Eq. 4.18, the apparent wind angle, $\phi(r)$, is calculated for a number of radial blade positions from $r = 0$ to $r = R$ in Fig. 4.4. Here, the wind turbine radius, R , is determined from the assumed required force to propel the boat upwind, whereas Eq. 4.20 and Eq. 4.21 are used to calculate the optimal $\phi(r)$ for other true wind angles, given the wind turbine radius, R . We see that it is not possible to obtain the exact optimal ϕ distribution in Fig. 4.4 for a given true wind angle, θ , by turning the blades a certain angle, if the blades are designed for e. g. optimal upwind performance.

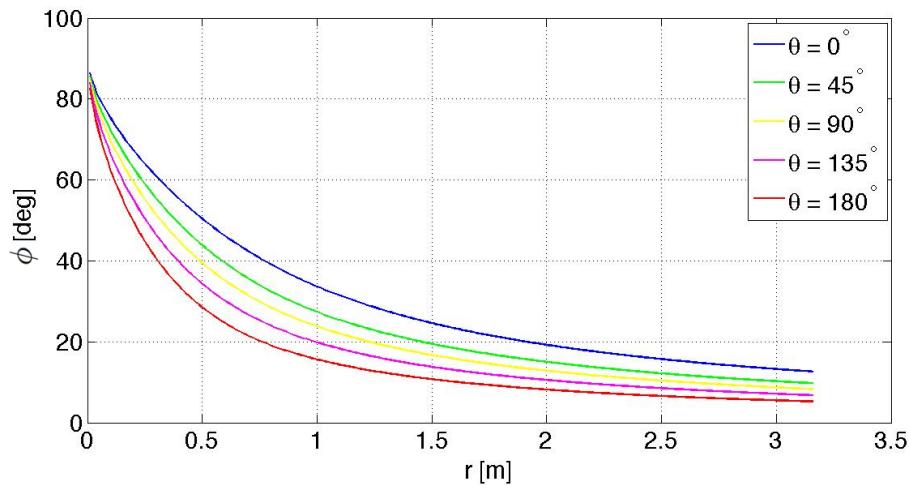


Figure 4.4: Apparent wind angle ϕ vs true wind angle θ .

Table 4.1 shows the optimal wind turbine rotation rate, Ω , when the radius is fixed from the optimal upwind design, and S is given by Eq. 4.21.

Wind direction [°]	Rotation rate [rad/s]
0	16.57
45	19.87
90	17.64
135	12.79
180	9.47

Table 4.1: Optimal wind turbine rotation rate.

4.3 Optimal blade chord distribution

By combining Eq. 4.4 and Eq. 4.6, we get an expression for the chord length

$$c = \frac{8\pi U^2 a(1-a)r}{NV^2(C_L \cos \phi + C_D \sin \phi)} \quad (4.22)$$

From Fig. 4.1 we have

$$\sin^2 \phi = \frac{U^2(1-a)^2}{V^2} \quad (4.23)$$

and by inserting this into Eq. 4.22 we get

$$c = \frac{8\pi r \sin^2(\phi)a}{N(C_L \cos \phi + C_D \sin \phi)(1-a)} \quad (4.24)$$

This is a different expression than what Blackford obtained for c .

If a NACA 4412 airfoil is used with $\epsilon = 0.03$, $C_L = 0.8$ and $C_D = 0.024$, at 4° angle of attack, are reasonable values. Fig. 4.5 shows the chord length for a four-bladed wind turbine with $C_L = 0.8$ and $C_D = 0.024$, calculated with Eq. 4.24, for the apparent wind angle distributions in Fig. 4.4. Of course, the chord length cannot be 0 at $r = 0$ from a strength perspective.

Knowing the blade design, the net force obtained with this blade design can now be found by numerical integration of Eq. 4.5 from $r = 0$ to $r = R$. The result of this integration should equal the assumed required net force that the blade design is based on. Numerical integration gives $F_{net} = 2046$ N, which is a fairly good result. In (Blackford, 1985a), Blackford assumed a required net force of 600 N, and numerical integration of Eq. 4.5 resulted in $F_{net} = 650$ N.

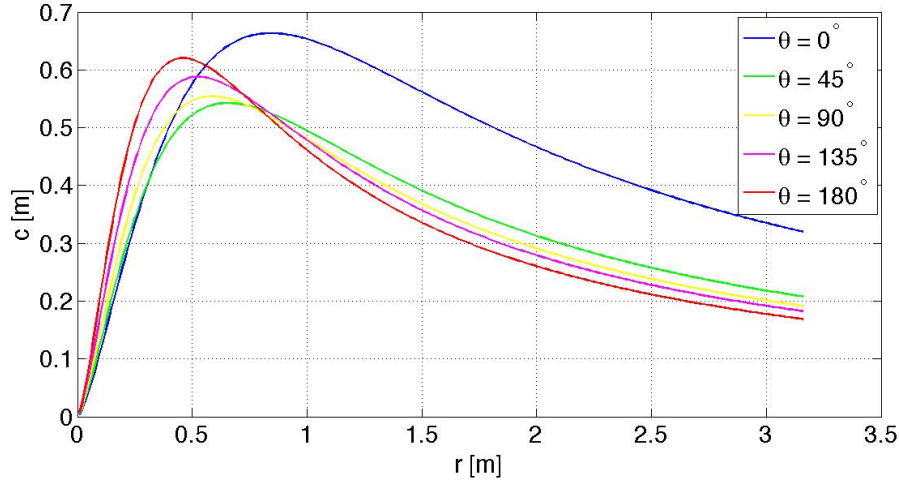


Figure 4.5: Chord distribution.

4.4 Correction for a finite number of blades

In the blade design procedure described above, it is assumed that the number of blades is infinite. As discussed by Glauert (Glauert, 1943), the maximum velocity reduction in the slipstream, $2Ua$, see Appendix A.1, only occurs on the vortex sheets formed by the trailing vortices from the blade tips. The circumferential average decrease of axial velocity in the slipstream is only a fraction F of this velocity. The wind speed reduction parameter a should therefore be multiplied with F to account for a finite number of blades, N . An approximate expression for F was first worked out by Prandtl, known as Prandtl's tip loss factor:

$$F = \frac{2}{\pi} \arccos [\exp(-f)] \quad (4.25)$$

where

$$f = \frac{N}{2} (1 - s/S) \sqrt{1 + S^2} \quad (4.26)$$

Later, Goldstein worked out a complex but more accurate expression for F , shown graphically in Fig. 4.6 for a four-bladed propeller. The influence of Prandtl and Goldstein's correction factors on the blade design is shown in Table 4.2. We see that the correction factors only influence the blade design near the blade tip, and that the difference in blade design is small between the Prandtl corrected design and the Goldstein corrected design.

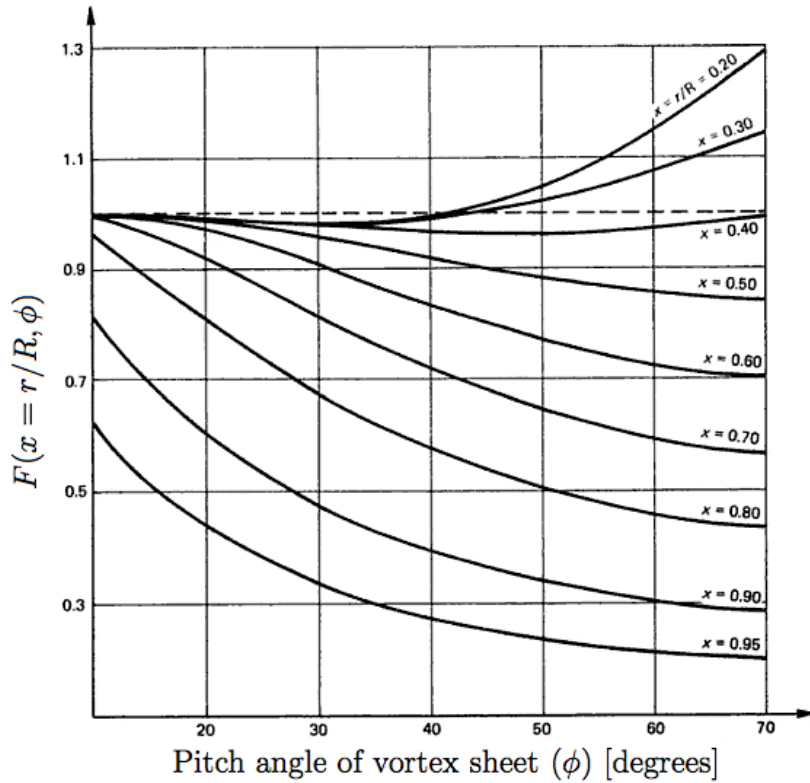


Figure 4.6: Goldstein factors for four-bladed propellers. Modified from (Carlton, 2007).

		Uncorrected		Prandtl			Goldstein		
r/R	r	ϕ	c	F	ϕ	c	F	ϕ	c
0.20	0.63	44.9	0.634	1.00	45.0	0.633	1.00	44.9	0.634
0.30	0.95	34.9	0.658	1.00	34.9	0.657	1.00	34.9	0.658
0.40	1.27	28.1	0.609	0.99	28.2	0.605	1.00	28.1	0.609
0.50	1.58	23.6	0.546	0.98	23.7	0.539	0.99	23.6	0.542
0.60	1.90	20.1	0.484	0.97	20.3	0.472	0.97	20.3	0.473
0.70	2.22	17.5	0.431	0.93	17.8	0.408	0.94	17.8	0.412
0.80	2.53	15.5	0.388	0.85	16.1	0.344	0.83	16.2	0.337
0.90	2.85	13.9	0.350	0.68	15.1	0.259	0.63	15.3	0.243
0.95	3.01	13.2	0.334	0.51	14.9	0.193	0.47	15.1	0.180

Table 4.2: Influence of Prandtl and Goldstein corrections on blade design.

The power from the wind turbine, the thrust on the wind turbine, and the net forward force from the wind turbine are calculated by numerical integra-

tion of Eq. 4.7, Eq. 4.4, and Eq. 4.5 respectively. The results are shown in Table 4.3 for the uncorrected blade design, and the Prandtl factor corrected blade design. The numerical integration is not carried out for the Goldstein corrected blade design, because the Goldstein factors are only found here for the given r/R values in Fig. 4.6. However, it is believed that P , F_W , and F_{net} from the Goldstein factor corrected blade design will vary only slightly from the same values found using the Prandtl factor corrected blade design, due to the quite small deviation between the Prandtl factor and the Goldstein factor, see Table 4.2.

	P [W]	F_W [N]	F_{net} [N]
Uncorrected	28116	2734	2046
Prandtl	25033	2338	1917

Table 4.3: Influence of Prandtl's tip loss factor on wind turbine performance.

We see from Table 4.2 that F_{net} from the Prandtl factor corrected blade design is 6% less than F_{net} from the uncorrected blade design. Using the Prandtl tip loss factor in the blade design procedure, the wind turbine radius must be increased by 2.2% in this case, compared to the uncorrected wind turbine radius, to obtain but the required F_{net} .

5 Use of wind turbines on ships

5.1 What type of wind turbine?

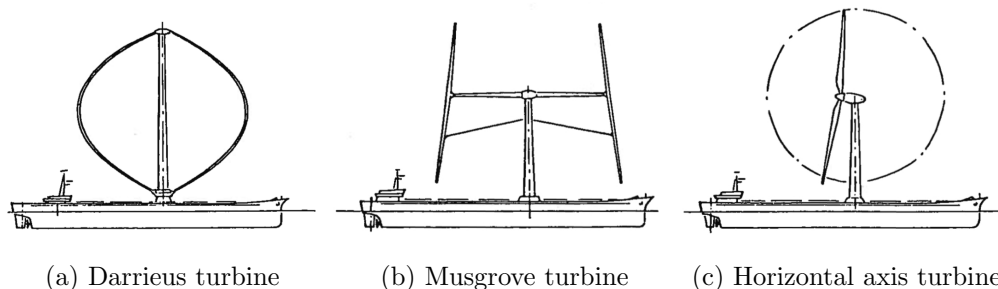
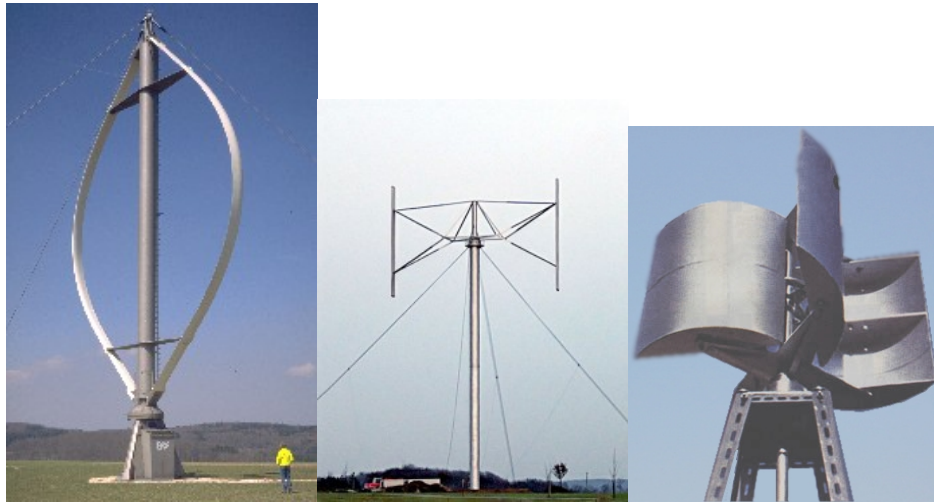


Figure 5.1: Different suggestions for windmill ships (Bose, 1980).

One of the first questions that comes to mind when considering wind turbines on a ship for ship propulsion, is what kind of wind turbine design should one choose? There is a wide range of different wind turbine designs, but the designs can normally be categorized as either horizontal-axis wind turbines (HAWT) or vertical-axis wind turbines (VAWT), see Fig. 5.1. The difference between these two categories is the direction of the rotating axis of the wind turbine.

While there is not much variation in the design of the horizontal-axis wind turbine, the vertical-axis wind turbine comes in numerous variants. The most common types of VAWTs are shown in Fig. 5.2: Darrieus, giromill (of which the Musgrove wind turbine in Fig. 5.1b is a variant), and Savonius wind turbines.

The Darrieus wind turbine consists of two or three curved slender airfoils, mounted in each end of a vertical rotating shaft. A subtype of the Darrieus turbine is the giromill, with straight, as opposed to curved, blades. The giromill generally has a higher coefficient of performance, see Eq. 5.2, than the Darrieus turbine, and is more efficient in turbulent winds (Wikipedia, 2010). The Savonius wind turbine is a VAWT with scoops acting as drag devices, and is mainly used when cost and reliability is more important than efficiency. Because the majority of the rotating mass is located far from the shaft, vertical-axis wind turbines experience very high centrifugal stresses,



(a) Darrieus (Renewable Energy UK, 2010) (b) Giromill (EnergyBeta, 2010) (c) Savonius (The green energy website, 2010)

Figure 5.2: Three different types of VAWTs.

and guy-wires are often required to stabilize the structure. This feature makes VAWTs difficult to employ on a slender ship.



Figure 5.3: Diffuser-Augmented Wind Turbine (Wind-Works, 2010).

The Diffuser-Augmented Wind Turbine (DAWT), see Fig. 5.3, is an interesting wind turbine design, due to various claims of increased power output compared to a conventional bare turbine. The DAWT will benefit from a lower thrust force on the rotor, than a HAWT with the same power output, due to increased velocity at the rotor disc. This can be seen from the efficiency of a wind turbine, defined in Eq. 5.1, where Q is the torque, Ω is the angular frequency, T is the thrust, and U_t is the velocity at the rotor disc. The power output from the wind turbine is $P = Q\Omega$.

$$\eta_t = \frac{Q\Omega}{TU_t} \quad (5.1)$$

The increased velocity at the rotor disk allows for a smaller turbine diameter than a HAWT at the same power output, resulting in reduced thrust, lower torque and higher rotational speed.

The lower thrust and torque levels yield a lighter center-body, which is positive from a structural and economic point of view. The diffuser reduces blade tip-losses, which is the primary source of noise, and it also reduces sensitivity to yaw-misalignment (Phillips, 2003).

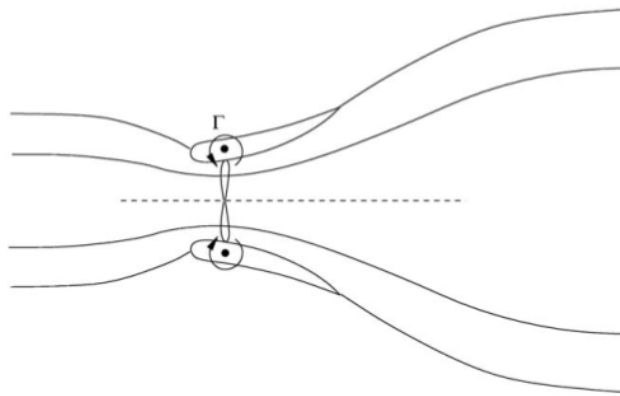


Figure 5.4: Ideal flow through a wind turbine in a diffuser (Hansen, 2008).

As Fig. 5.5 shows, placing the wind turbine in a diffuser will increase the power output significantly for the same thrust, compared to a bare turbine. The power coefficient or coefficient of performance, C_P , is defined as

$$C_P = \frac{P}{\frac{1}{2}\rho_a U^3 A_t} \quad (5.2)$$

whereas the thrust coefficient, C_T , is defined as

$$C_T = \frac{T}{\frac{1}{2}\rho_a U^2 A_t} \quad (5.3)$$

A good reason for using DAWTs onboard ships is its protected wind turbine, which results in noise reduction and a safe working environment for the crew working on deck. The downside is increased drag due to the diffuser, higher cost and weight. Increased weight often leads to a larger supporting structure which again leads to higher drag than a conventional bare turbine.

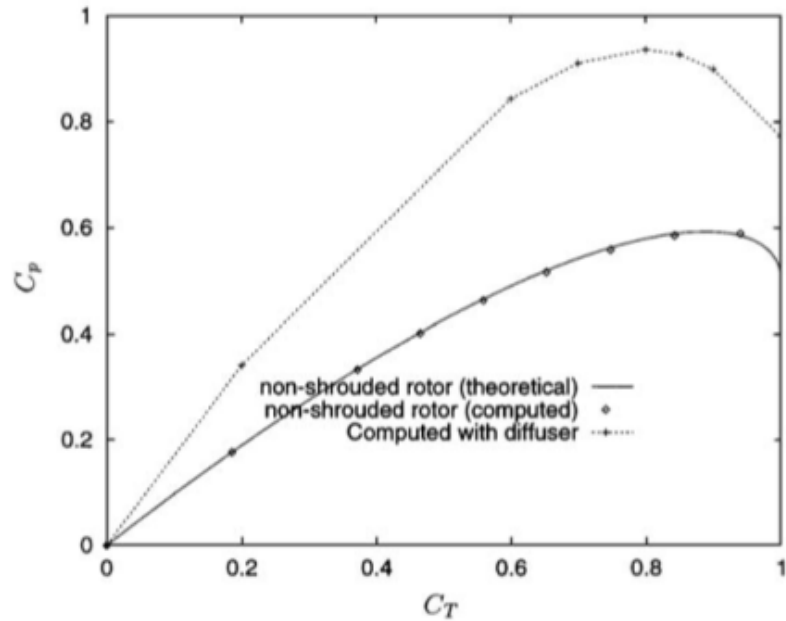


Figure 5.5: Computed power coefficient C_p for a rotor in a diffuser as a function of the thrust coefficient C_T (Hansen, 2008).

The structural load during an extreme wind situation is also increased compared to a bare turbine. Derek Grant Phillips concludes in his PhD-thesis on diffuser-augmented wind turbines (Phillips, 2003) that “DAWTs are uneconomic compared to HAWTs, and will remain so until there is a breakthrough in the design to reduce drag at the peak wind speed.” The increased drag due to the diffuser and supporting structure should be studied further to conclude whether or not the increased power output exceeds the power to overcome the increased resistance, if a DAWT is used onboard a ship.

Based on the discussion above, the conventional HAWT seems to be the most feasible design for a wind turbine propelled ship. HAWT is also the design used on nearly all, if not all, well documented full-scale wind turbine boats that have been built.

5.2 Comparison against other forms of wind-assisted ship propulsion

Using the theory outlined in Sec. 4.1, Blackford compared the net forward thrusts produced by wind turbine propulsion and by airfoil sails, also known as wingsails. When the notation from Sec. 4.1 is used, an airfoil of area A with an angle θ' to the apparent wind U , produces a lift force perpendicular to the apparent wind

$$F_L = \frac{1}{2}\rho_a C_L A U^2 \quad (5.4)$$

where C_L is the lift coefficient of the airfoil, and a drag force parallel to U

$$F_D = \frac{1}{2}\rho_a C_D A U^2 \quad (5.5)$$

where C_D is the drag coefficient of the airfoil.

The net force propelling the boat forward is then

$$F_{net} = F_L \sin \theta' - F_D \cos \theta' \quad (5.6)$$

In order to compare the forward force from wingsails with the forward force from wind turbine propulsion, the normalized forward force is computed:

$$\frac{F_{net}}{\rho_a A W^2} = \frac{1}{2} \left(\frac{U}{W} \right)^2 [C_L \sin \theta' - C_D \cos \theta'] \quad (5.7)$$

C_L and C_D will vary with apparent wind angle θ' , because the airfoil is rotated to obtain maximum forward force in all wind directions. The following values of C_L and C_D are taken from (Marchaj, 1964), and are about the best one could hope for:

$$\text{For } 0^\circ < \theta' < 90^\circ, C_L = 1.5 \text{ and } C_D = 0.3$$

$$\text{For } 90^\circ < \theta' < 180^\circ, C_L = 1.5(1 + \cos \theta') \text{ and } C_D = 0.3 - \cos \theta' \quad (5.8)$$

The net forward force from the wind turbine propulsion is also divided by $\rho_a A W^2$, where $A = \pi R^2$, i. e. the rotor disk area of the wind turbine, in order to compare the forward force from wingsails with the forward force from wind

turbine propulsion. It was assumed that the absolute best possible efficiency factor of the driving mechanism, ζ , and lift-to-drag ratio, ϵ , are $\epsilon = 0.01$ and $\zeta = 0.95$. The optimal wind speed reduction factor, a_0 , and the tip speed ratio, S , are for different true wind angles, θ , given by Eq. 4.20 and Eq. 4.21.

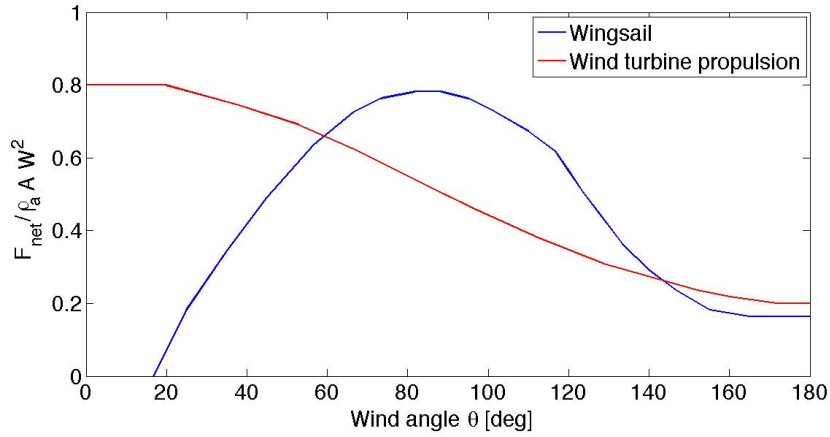


Figure 5.6: Normalized net forward force versus true wind angle, θ , for wingsail and wind turbine propulsion, $f = 0.5$. Modified from (Blackford, 1985a).

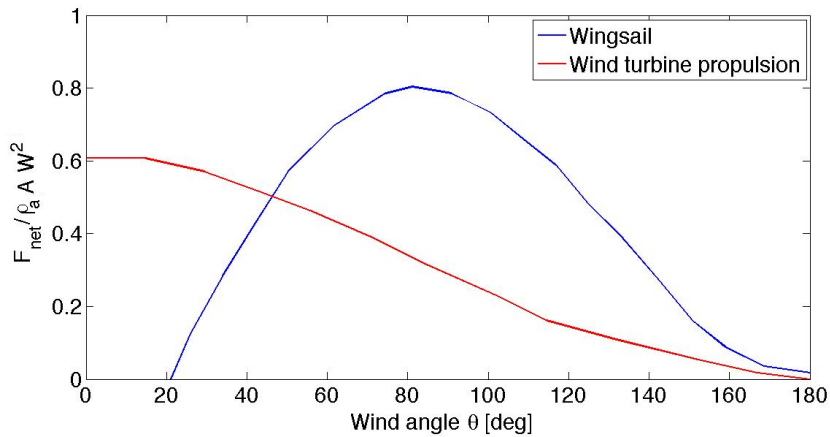


Figure 5.7: Normalized net forward force versus true wind angle, θ , for wingsail and wind turbine propulsion, $f = 0.75$. Modified from (Blackford, 1985a).

Fig. 5.6 and 5.7 show the forward force of the two propulsion systems, under the aforementioned assumptions, compared to each other for different true wind angles, for $f = 0.5$ and $f = 0.75$. Wind turbine propulsion will always be superior to wingsail propulsion for wind angles close to headwind, but in

general, it can be concluded that for values of $f \gtrsim 0.5$, wingsail propulsion is superior to wind turbine propulsion for most wind angles, and that the opposite is true for $f \lesssim 0.5$.

Fig. 5.8 shows the required auxiliary power to propel ships with different forms of wind-assisted propulsion for true wind angles from 0° (headwind) to 180° (downwind), for a ship speed of 6 m/s and a wind speed of 12 m/s. The ship used in the calculations is the MV St Helena, a 100 m long cargo/passenger vessel, and the route used in the calculations is UK - Las Palmas - Ascension - St Helena - Cape Town (Rainey, 1980). For this wind and ship speed, the wind turbine excels as the form of wind-assisted ship propulsion which requires the least auxiliary power, when all wind angles are considered.

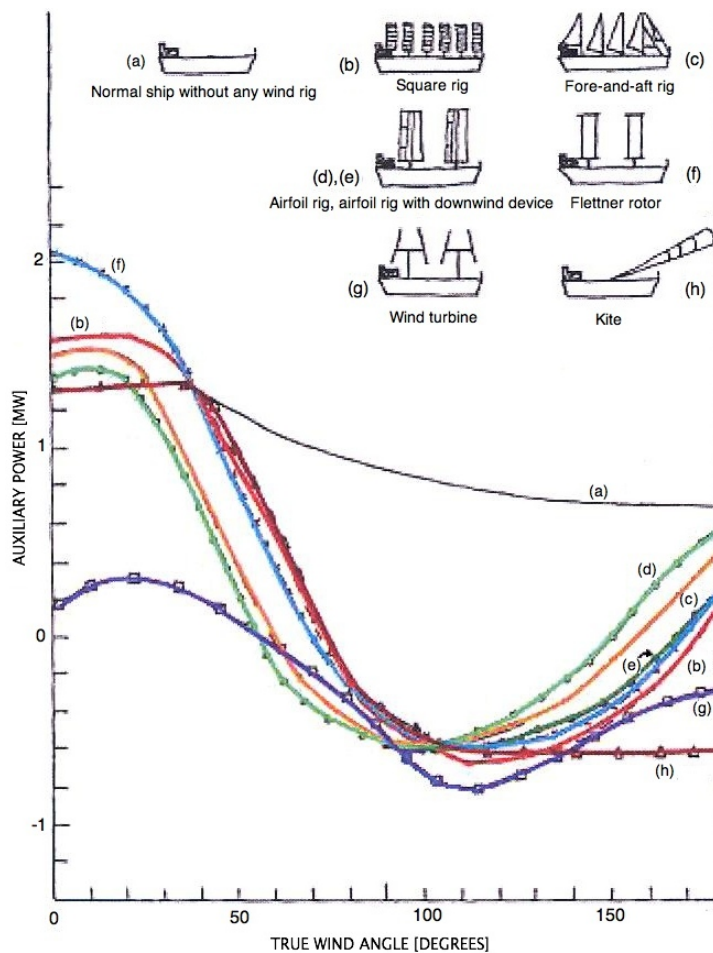


Figure 5.8: Fuel power required for ships with wind rigs. Modified from (Nance, 1985; Rainey, 1980).

Table 5.1 shows the true wind directions, θ , and ship speed to wind speed ratios, f , for which various forms of wind-assisted ship propulsion can operate. $\theta = 0^\circ$ represents headwind. The so-called mechanically assisted high-lift device, M, in Table 5.1, is a device that uses external energy to generate lift, such as the rotating cylinder, known as the Flettner rotor.

The wind turbine propelled ship is the only wind-assisted ship that can sail at all wind angles without auxiliary power, but only for low ship speeds compared to the wind speed. The rigid airfoil, also known as wingsail, can be used to sail closer to headwind than conventional soft sails ($\theta = 30 - 60^\circ$), and also faster for $\theta = 60 - 90^\circ$. If maintaining a given route and transit speed is the overall goal for a ship operator, based on Table 5.1, a combination of wind turbine(s) and airfoils seems to be the most fuel-saving option. Sailing headwind in narrow inlets and channels where tacking is not an option, the wind turbine will generate auxiliary propulsive power, while at other angles to the wind, the wingsails will be the main mean of propulsion. By employing a wind turbine onboard a ship, power may also be generated when the ship is in harbor, which can be stored and used when necessary.

f	True wind heading angle θ [°]					
	0-30	30-60	60-90	90-120	120-150	150-180
0.0-0.5	W	A W	A K M S W	A K M S W	A K M S W	A K M S W
0.5-1.0			A S	A K M S	A K M S	A K M S
1.0-1.5			A	A M S	A S	
Key: A = rigid airfoil, K = kite, M = mechanically assisted high-lift device, S = soft sail, W = wind turbine						

Table 5.1: Wind-assisted propulsion performance envelope chart (Bose, 2008).

5.3 Fuel savings for a notional wind turbine ship

In order to give an estimate on the fuel savings for a ship using a wind turbine for auxiliary power generation, a notional wind turbine ship is set to sail the route Peterhead - Bremerhaven - Peterhead, see Fig. 5.9. This route is chosen primarily due to the weather stations in close proximity to the route, for which statistical wind data is available. The route is divided into 8 legs, where the wind data for each leg is taken from the closest weather station.

Table 5.2 gives the dominant wind directions and average wind speeds for the different legs in January.



Figure 5.9: The route for the wind turbine ship.

Leg	Distance	Weather station	Dominant wind direction	Average wind speed [m/s]
Peterhead - b	63.01 km	Peterhead Harbour	SxSW	6.7
b - c	150.26 km	Forties 3 Platform	SxSW	9.3
c - d	144.97km	Ekofisk Platform	SxSW	12.9
d - e	140.62km	Tyra Oest	ExSE	12.9
e - f	118.39 km	Nordseeboje 2	ExSE	9.8
f - g	91.36 km	Feuerschiff Dt. Bucht	N	9.8
g - h	48.15 km	Leuchtturm Alte Weser	SE	10.3
h - Bremerhaven	29.65 km	Bremerhaven	SxSW	6.2

Table 5.2: Route with wind data (Windfinder, 2010).

The wind speed is typically given at a reference height of 10 m above the ground/water. To calculate the local wind speed at elevation z , Eq. 5.9 can

be used (Myrhaug, 2006):

$$\bar{U}(z) = \bar{U}_{10} \left(\frac{z}{10} \right)^\alpha \quad (5.9)$$

where $\bar{U}(z)$ is the mean wind speed at elevation z , \bar{U}_{10} is the mean wind speed at 10 m elevation, and $\alpha = 1/7 = 0.1429$ is a typical value of α . In the following calculations, however, a uniform velocity profile, based on the wind speeds in Tab. 5.2, is used. This simplifies the calculations of the drag on the wind turbine tower, but it also means that the wind speeds used in the calculations are lower than in reality, for the route and time of year considered here. For example, at a height of 72 m above the waterline, the wind speed is 13.3 m/s if the wind speed is 10 m/s at 10 m elevation.

Axial momentum theory assumes that the flow velocity is uniformly distributed in the radial direction of the stream. It is thus questionable if axial momentum theory can be used for the large wind turbine considered in the following calculations. Nevertheless, axial momentum theory is used in the following as a simple tool for calculating the fuel savings for a wind turbine ship. In Sec. 5.4, the more advanced blade element momentum theory is used to calculate the fuel savings for an optimized version of the wind turbine ship.

Length on waterline	325.503 m
Breadth on waterline	58.001 m
Draught at $L_{pp}/2$	20.800
Depth to 1st deck	28.015 m
Block coefficient	0.8100
Volume displacement	312693.3 m ³

Table 5.3: Main dimensions of the wind turbine ship.

The ship chosen is a VLCC with the main dimensions given in Table 5.3. More details on the VLCC can be found in the hydrostatics report and resistance curve from the program ShipX, found in Appendix B, as well as at http://www.gothenburg2010.org/kvlcc2_gc.html.

The wind turbine chosen to be used onboard the ship is the Vestas V90 wind turbine, with key data given in Table 5.4 (Vestas, 2009), and power curve, see Fig. 5.10.

Using the theory described in Sec. 2.4, the net power from the wind turbine is calculated for different wind directions at different wind speeds, when the

Rotor diameter	90 m
Hub height	65 m
Hub diameter	3.6 m
Rated power	3,000 kW
Cut-in wind speed	3.5 m/s
Rated wind speed	15 m/s
Cut-out wind speed	25 m/s
Maximum chord length	3.5 m

Table 5.4: Vestas V90 key data.

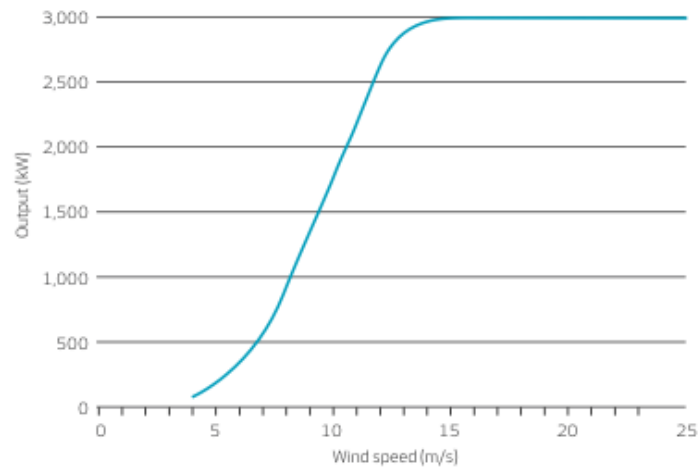


Figure 5.10: Vestas V90 power curve (Vestas, 2009).

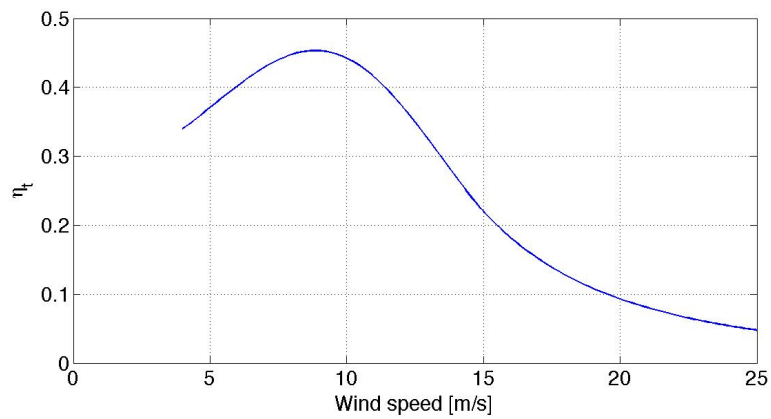


Figure 5.11: Vestas V90 efficiency.

ship is sailing at 15 kn and the total efficiency factor is $\zeta = 0.7$, in Fig. 5.12. The net power from the wind turbine is defined as power generated by the wind turbine minus power required to overcome the added air resistance due to the thrust force on the wind turbine rotor disk and the drag on the wind turbine tower. The required power to overcome the added air resistance is the resistance force times the ship speed, divided by the total efficiency factor ζ . When the wind is from the aft, the wind turbine tower will act as a drag device and will together with the thrust on the wind turbine work as a propulsive force. The efficiency of the Vestas V90, see Fig. 5.11, is found from the power curve as

$$\eta_t = \frac{P}{\frac{1}{2}\rho_a U^3 A_t} \quad (5.10)$$

where P is the power found from the power curve at a given wind speed.

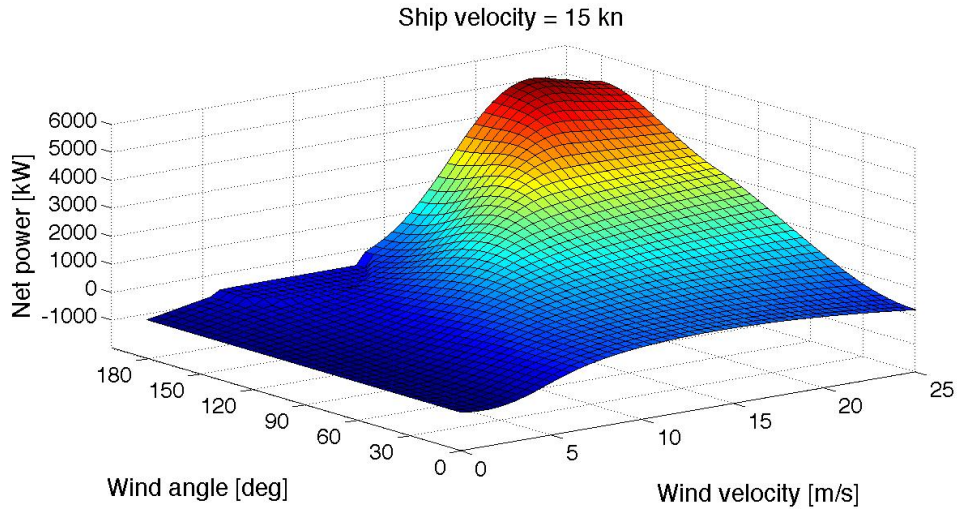


Figure 5.12: Net power from a Vestas V90 wind turbine for a ship sailing at 15 kn.

The journey Peterhead - Bremerhaven - Peterhead is 1573 km long and takes 56.62 hours at a ship speed of 15 knots. Lower ship speed in and out of the harbors is not accounted for here. With a resistance at 15 kn of 1834 kN, and a total efficiency factor $\zeta = 0.7$, the required engine power is 20.216 MW. The total energy consumed over the journey is thus

$$E_{tot} = 56.62 \text{ h} \cdot 20216 \text{ kW} = 1,144,630 \text{ kWh} \quad (5.11)$$

Table 5.5 gives the total energy saved with the wind turbine onboard for the route, when the ship is sailing at 15 kn. It is assumed that the engine

power can be replaced with electric power from the wind turbine, through a diesel-electric propulsion system. The total energy saved with the wind turbine onboard is 41,531.1 kWh, or 149,512.0 MJ, i. e. 3.6% of the total fuel energy. With a calorific value of 44 MJ/kg for diesel fuel, the fuel saving for one Peterhead - Bremerhaven - Peterhead trip in January with a Vestas V90 onboard, sailing at 15 knots, will be 3398 kg.

Leg	Wind angle relative to ship [deg]	Wind speed [m/s]	Net power from Vestas V90 [kW]	Time in leg per voyage [h]	Energy saved per voyage [kWh]
Peterhead - b	82.6	6.7	36.3	2.268	82.4
b - c	82.6	9.3	818.8	5.409	4428.8
c - d	82.6	12.9	1529.6	5.219	7983.0
d - e	7.9	12.9	691.8	5.062	3501.7
e - f	7.9	9.8	573.2	4.262	2443.1
f - g	120.4	9.8	676.9	3.289	2226.3
g - h	14.6	10.3	618.0	1.733	1071.0
h - Bremerhaven	82.6	6.2	-94.1	1.067	-100.4
Bremerhaven - h	97.4	6.2	-151.7	1.067	-161.8
h - g	165.4	10.3	0.1	1.733	0.1
g - f	59.6	9.8	825.1	3.289	2713.6
f - e	172.1	9.8	0.9	4.262	3.7
e - d	172.1	12.9	762.0	5.062	3857.0
d - c	97.4	12.9	1827.0	5.219	9535.2
c - b	97.4	9.3	747.7	5.409	4044.3
b - Peterhead	97.4	6.7	-42.7	2.268	-96.9
Sum				56.62	41531.1

Table 5.5: Energy savings for the North Sea route at 15 kn.

Reducing the sailing speed from 15 kn to 10 kn reduces the resistance from 1834 kN to 844 kN, hence reducing the engine power from 20.216 MW to 6.202 MW, with a total efficiency factor of 0.7. Table 5.6 gives the total energy saved with the wind turbine onboard for the route, when the ship is sailing at 10 kn.

With a required engine power of 6.202 MW, the total energy consumed over

Leg	Wind angle relative to ship [deg]	Wind speed [m/s]	Net power from Vestas V90 [kW]	Time in leg per voyage [h]	Energy saved per voyage [kWh]
Peterhead - b	82.6	6.7	417.5	3.402	1420.5
b - c	82.6	9.3	1268.3	8.114	10291.4
c - d	82.6	12.9	2160.7	7.829	16915.8
d - e	7.9	12.9	1406.7	7.593	10681.3
e - f	7.9	9.8	1211.7	6.393	7746.7
f - g	120.4	9.8	1077.1	4.934	5314.5
g - h	14.6	10.3	1272.0	2.600	3307.2
h - Bremerhaven	82.6	6.2	296.0	1.601	473.9
Bremerhaven - h	97.4	6.2	233.0	1.601	373.1
h - g	165.4	10.3	599.1	2.600	1557.7
g - f	59.6	9.8	1421.6	4.934	7014.1
f - e	172.1	9.8	420.5	6.393	2688.5
e - d	172.1	12.9	1795.0	7.593	13629.8
d - c	97.4	12.9	2416.5	7.829	18918.6
c - b	97.4	9.3	1163.6	8.114	9441.8
b - Peterhead	97.4	6.7	337.5	3.402	1148.0
Sum				84.93	110922.9

Table 5.6: Energy savings for the North Sea route at 10 kn.

the journey that takes 84.93 hours is

$$E_{tot} = 84.93 \text{ h} \cdot 6202 \text{ kW} = 526,736 \text{ kWh} \quad (5.12)$$

We see that reducing the ship speed from 15 to 10 knots will itself reduce the total amount of fuel consumed over the journey by 54%.

The total energy saved with the wind turbine onboard, see Table 5.6, is 110,922.9 kWh, or 399,322.4 MJ, i. e. 21.1% of the total fuel energy. The fuel saving for the route in January, sailing at 10 knots, will be 9076 kg.

5.4 Optimized notional wind turbine ship

Now, let us use the optimal blade theory from Sec. 4 in designing the wind turbine blades, and study the fuel savings for the optimized notional wind turbine ship. The radius of the wind turbine is set to $R = 45$ m in order to compare the optimized wind turbine ship with the wind turbine ship of Sec. 5.3. ζ is set to 0.7 for the same reason. In the calculations for the optimized wind turbine ship, a four-bladed wind turbine is used, whereas the Vestas V90 wind turbine has three blades. The four-bladed wind turbine is chosen for the optimized wind turbine, because F_{net} is theoretically increasing with the number of blades, as shown in (Blackford, 1985a). The effect of increasing the blade number above four, however, is small. In order to compare the optimized wind turbine ship with the wind turbine ship in Sec. 5.3, where the axial momentum theory of Sec. 2.4 is used in the calculations, Prandtl's tip loss factor is neglected in the following calculations.

According to the theory in Sec. 4, for given values of θ, W, f and ζ , there is a value of a_0 that gives the maximum possible net forward force for a given radius R . In order for the wind turbine to operate at different values of a_0 , a different blade design is required for each combination of θ, W, f , if ζ is fixed. This is, of course, totally impractical, and a practical alternative is to use a wind turbine with controllable blade pitch. However, as shown in Fig. 4.4, it is not possible to obtain the optimal pitch for all radii if the blade is turned a certain angle from, say, the optimal upwind blade pitch. As Blackford points out, it would likely be best to design the wind turbine for optimal performance upwind, since this is the most important and most critical direction.

From the discussion above, and the fact that the wind turbine ship is set to sail in an approximate 10 m/s wind at 10 kn, which means that $f \approx 0.5$, the optimized wind turbine ship is designed for $\theta = 0$, $W = 10$ m/s and $f = 0.5$. It is still assumed that all blade sections operate at an angle of attack of $\alpha = 4^\circ$, and that $C_L = 0.8$ and $C_D = 0.024$. The chord distribution, see Fig. 5.13, and pitch angle distribution, see Fig. 5.14, is hence fixed from this blade design, but the blades can be turned, and Ω regulated by a gearing mechanism, to maximize F_{net} for the specific combination of θ, W , and f .

With the chord and pitch angle distributions known, the wind reduction

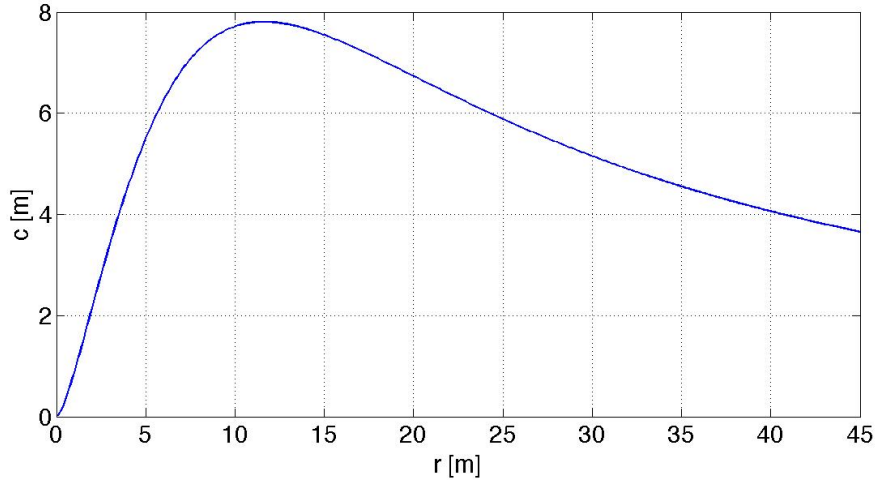


Figure 5.13: Blade chord distribution for the optimized wind turbine ship.

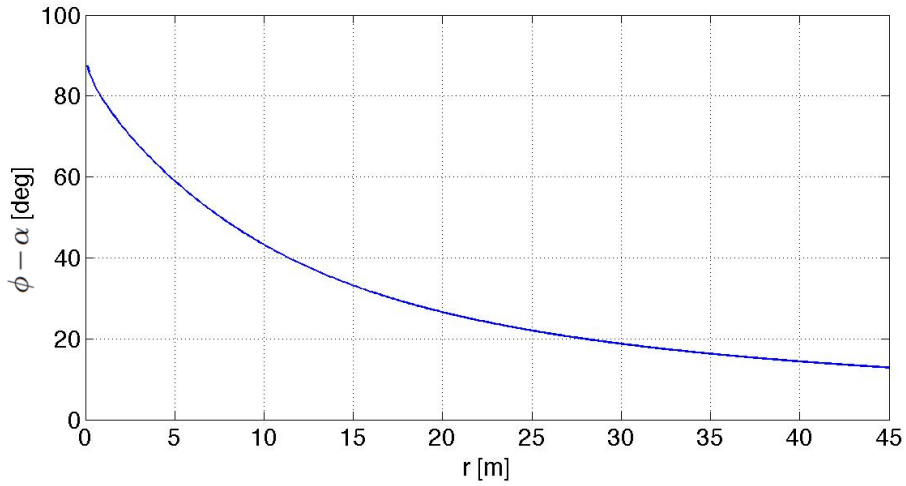


Figure 5.14: Blade pitch angle distribution, $\phi - \alpha$, for the optimized wind turbine ship.

factor, a , is now calculated from Eq. 4.24. Solving Eq. 4.24 for a yields

$$a = \frac{b}{1 + b} \quad (5.13)$$

where

$$b = \frac{cN(C_L \cos \phi + C_D \sin \phi)}{8\pi r \sin^2 \phi} \quad (5.14)$$

Knowing a , a' is then calculated from Eq. 4.14. We can now check if the

values of a , a' and Ω results in the correct ϕ , see Fig. 4.1. An iteration procedure must be performed for different angles of attack α at each radial blade position, to find the α which gives the correct ϕ . Using the NACA 4412 foil section, C_L as a function of α is given in (Abbott and von Doenhoff, 1959), and it is assumed that $C_D = \epsilon C_L$, where $\epsilon = 0.03$ still is used.

Table 5.7 shows the maximum F_{net} one will have at each leg of the journey, when designing the blades for $\theta = 0$, $W = 10$ m/s, and $f = 0.5$. Ω is adjusted, and the blades are turned a certain angle from the design position, to maximize F_{net} at each leg. As Table 5.7 shows, using C_L as a function of α and $C_D = \epsilon C_L$, the resulting angle that the blade is turned for optimal performance is almost constant for each combination of θ , W , and f . For comparison reasons, the optimal a_0 and the resulting F_{net} if the blades were designed to be optimal for each leg of the journey, is also shown in Table 5.7. We see that by adjusting the rotation rate Ω and blade angle, for a given blade design, we can get relatively close to the optimal F_{net} if the blades were designed specifically for the actual values of θ , W , and f . F_{net} is found through numerical integration of Eq. 4.5.

In order to compare Table 5.7 with Table 5.6, the net power for Table 5.7 can be calculated by multiplying the net force with the ship speed and divide by the overall efficiency factor, $\zeta = 0.7$. This is the engine power that is saved when the wind turbine is used for auxiliary propulsion. The total energy saved using the optimized blade design for $\theta = 0$, $W = 10$ m/s, and $f = 0.5$, when adjusting the wind turbine rotation rate and blade angle, is 136,516.1 kWh. This equals 25.9% of the total required energy. The calculations for the optimized wind turbine ship does not include the effect of drag on the wind turbine tower, due to the complexity of radially varying induced axial and tangential velocities in the blade element theory. If the effect of drag on the wind turbine tower also is neglected from the analysis for the ship carrying a Vestas V90 wind turbine in 10 kn, the resulting energy saved is 117,524,9 kWh, which equals 22.3% of the total required energy.

To further see the effect of optimizing the blade design: If the ship were to always sail at $\theta = 0$, $W = 10$ m/s and $f = 0.5$, the optimized wind turbine would provide 30.8% of the required power, whereas the Vestas V90 wind turbine would provide only 23.8% of the required power. The drag on the wind turbine tower is also here neglected when calculating the required power for both wind turbines.

Leg	Optimal a_0	Optimal Ω with original blade design	Optimal angle that blades are turned from original design [°]	$F_{net}[N]$ using optimal blade design	Maximum $F_{net}[N]$ achieved with original blade design
Peterhead - b	0.16	0.88	-7.45	3.83e4	3.63e4
b - c	0.22	1.10	-7.46	1.55e5	1.40e5
c - d	0.28	1.42	-7.47	4.94e5	4.15e5
d - e	0.22	1.77	-7.47	5.73e5	5.28e5
e - f	0.18	1.47	-7.45	2.34e5	2.22e5
f - g	0.32	0.83	-7.45	1.57e5	1.19e5
g - h	0.18	1.51	-7.46	2.75e5	2.60e5
h - Bremerhaven	0.13	0.77	-7.68	2.57e4	2.47e4
Bremerhaven - h	0.15	0.74	-7.45	2.12e4	2.00e4
h - g	0.44	0.54	-7.46	1.44e5	8.74e4
g - f	0.2	1.29	-7.47	2.08e5	1.93e5
f - e	0.45	0.46	-7.51	1.11e5	6.42e4
e - d	0.42	0.77	-7.46	3.52e5	2.19e5
d - c	0.29	1.30	-7.47	4.71e5	3.77e5
c - b	0.25	0.98	-7.47	1.44e5	1.24e5
b - Peterhead	0.17	0.77	-7.48	3.29e4	3.13e4

Table 5.7: Design parameters for the optimized wind turbine ship.

Fig. 5.15 shows the available force to overcome the ship resistance, F_{net} , as a function of ζ , when the wind turbine diameter is fixed at 90 m, using the theory from Sec. 4. It is clear that the overall propulsive efficiency has a tremendous influence on the fuel savings, since the resistance at 10 kn is 844 kN.

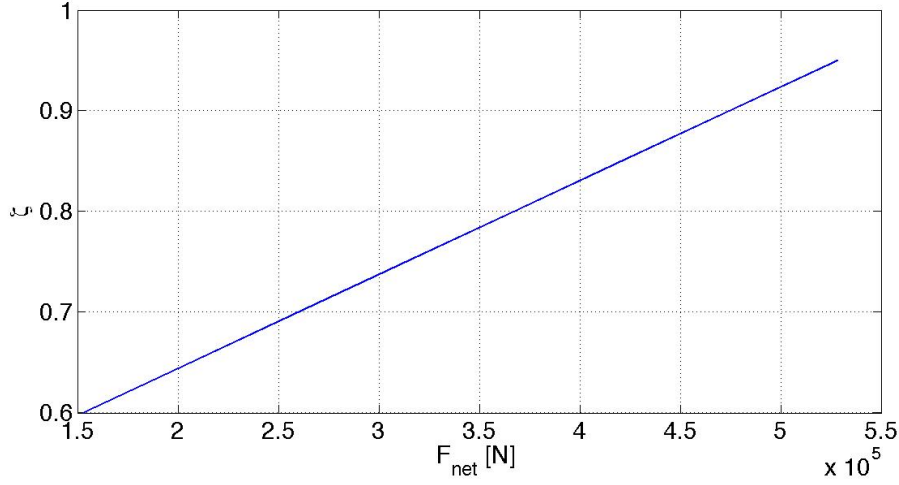


Figure 5.15: F_{net} as a function of ζ . $\theta = 0$, $W = 10$ m/s, and $f = 0.5$.

5.5 Considerations on a wind turbine propelled ship

The Vestas V90 wind turbine has a diameter of 90 m, making it at least 90 m tall. The blades must have a certain height above deck for safety reasons, and with a hub height of 65 m, the total height of the wind turbine is 110 m.

The following stability analysis shows that the VLCC studied in Sec. 5.3 will have sufficient stability with the Vestas V90 wind turbine onboard:

The heeling moment about the center of gravity of the ship is

$$M_{heeling} = \rho_a Q \Delta U \sin \theta' \cos \phi (h_t + h_G) \quad (5.15)$$

$$\begin{aligned}
& + C_{D,mast} \frac{1}{2} \rho_a ((U - \Delta U) \sin \theta' \cos \phi)^2 A_{mast,covered} (h_{mid,covered} + h_G) \\
& + C_{D,mast} \frac{1}{2} \rho_a (U \sin \theta' \cos \phi)^2 A_{mast,uncovered} (h_{mid,uncovered} + h_G)
\end{aligned} \quad (5.16)$$

where ϕ is the heel angle, h_t is the hub height above deck, $h_{mid,covered}$ is the middle height above deck of the part of the mast that is covered by the wind turbine, $h_{mid,uncovered}$ is the middle height above deck of the uncovered part of the mast, and h_G is the distance from the deck to the center of gravity of the ship, see Fig. 5.16.

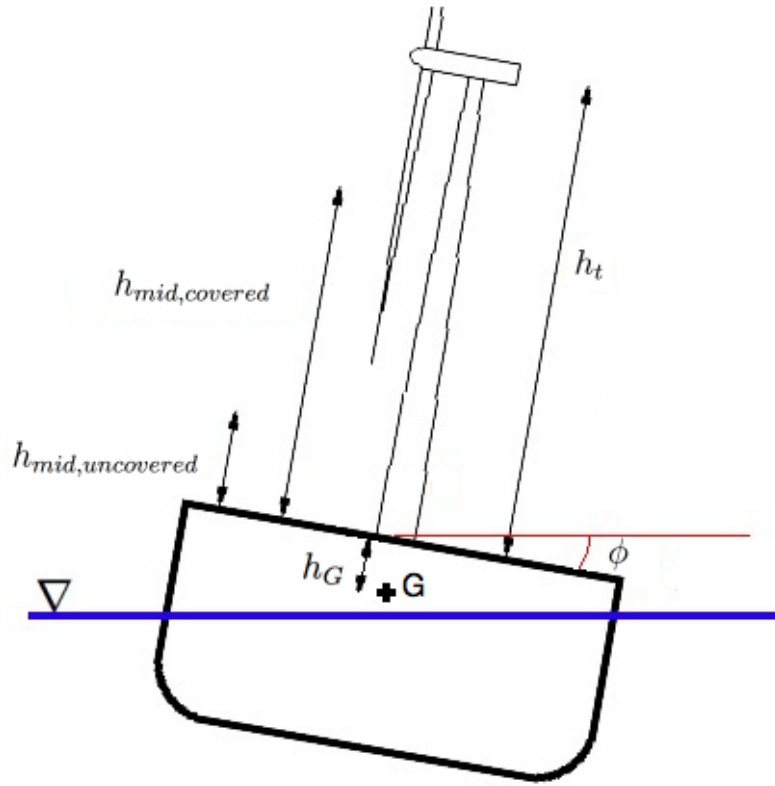


Figure 5.16: Heeling ship with heights explained.

The righting moment about the center of gravity of the ship is

$$M_{righting} = \rho_w \nabla g GZ \quad (5.17)$$

where ∇ is the volume displacement of the ship, and GZ is the righting arm, see Fig. 5.17, when the ship is heeling and the center of buoyancy moves from point B to point B_1 . With $KG = 18.6$ m, and $KM = 24.306$ m from the hydrostatics report from the program ShipX, see Appendix B, we have $GM = KM - KG = 5.706$ m. Then, GZ can be found as

$$GZ = GM \sin \phi \quad (5.18)$$

and we get

$$M_{righting} = \rho_w \nabla g GM \sin \phi \quad (5.19)$$

Fig. 5.18 shows the heeling and righting moments about the center of gravity of the ship when $\theta = 90^\circ$, the ship speed is zero, and the wind speed is 12.5 m/s. This is the wind speed that gives the highest heeling moment. The

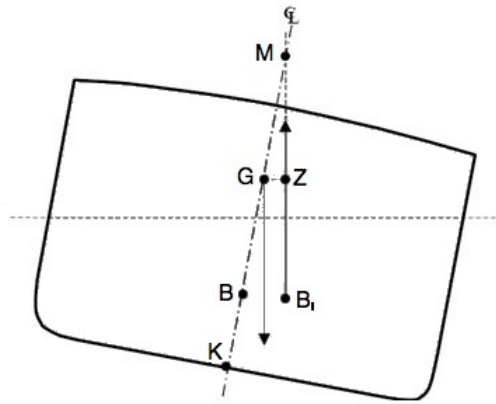


Figure 5.17: Ship stability notation.

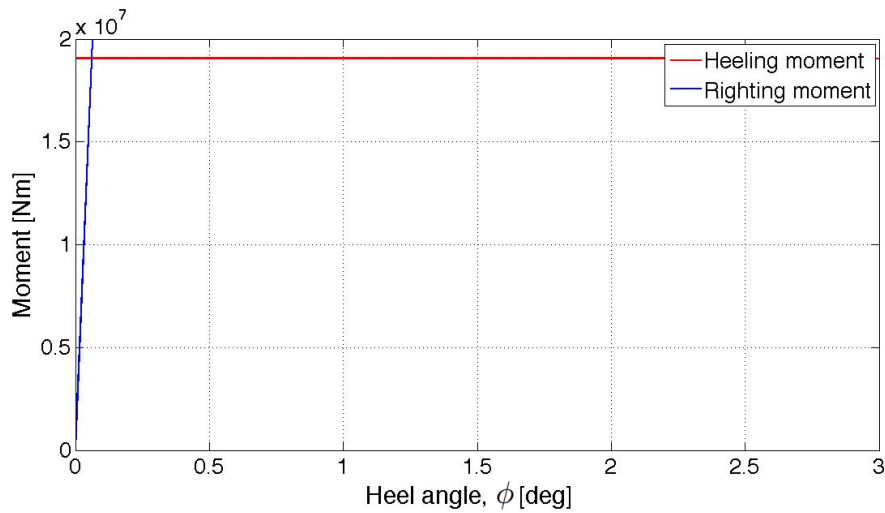


Figure 5.18: Heeling and righting moments in 12.5 m/s beam wind, zero ship speed.

highest heeling moment is $1.907 \cdot 10^7$ Nm. The center of gravity of the ship is 9.415 m below deck, $h_t = 65$ m, $h_{mid,covered} = 42.5$ m, and $h_{mid,uncovered} = 10$ m. When the righting moment equals the heeling moment, the ship will have a steady heel angle ϕ . This happens for $\phi = 0.061^\circ$. The optimized wind turbine design is based on maximizing the power output from the wind turbine while minimizing the thrust force on the wind turbine, so a higher heel angle will not occur for the optimized wind turbine ship.

The transverse force from the wind on the wind turbine must be balanced

by a lift force on the hull due to a leeway angle between the direction of the ship and its path, see Fig. 2.1. For such a small heel angle as $\phi = 0.061^\circ$, the leeway angle is negligible. However, for a smaller ship, where the transverse wind force is larger compared to the ship resistance, the leeway angle must be considered. To avoid that the wind turbine will give the ship a yaw moment, the wind turbine should be placed at the center of lift of the hull, which is about $0.22-0.23L_{pp}$ behind the forward perpendicular for the VLCC studied here, according to Prof. Tor Einar Berg at the Department of Marine Technology, Norwegian University of Science and Technology.

The Vestas V90 wind turbine with a 65 m high tower has a total weight of 219 tons (Vestas). The volume displacement of the oil tanker at the design waterline is $312,693.3 \text{ m}^3$ i. e. its weight is 320,511 tons. The Vestas V90 wind turbine will thus contribute to very little of the total weight of the ship, and it is justifiable to use the hydrostatic data for this loading condition.

The height of such a tall ship may be a problem, as it cannot sail the Panama Canal nor the Suez Canal. Furthermore, it cannot pass under the bridges that cross the seaward approaches to major ports such as San Francisco and New York. The height issue is a limiting factor for both wind turbine ships and ships equipped with soft or rigid sails (wingsails), and makes it very unpractical for such ships to have a total height of more than about 55 m, unless the wind turbine tower, wingsails or masts can be folded down somehow. A foldable mast will, however, increase the cost of the wind turbine rig.

Reducing the height of the ship by having several smaller wind turbines instead of one big wind turbine, is a possibility. The smaller wind turbines will, however, cover each other for certain wind directions, which will reduce the power output. This can be avoided by placing the wind turbines on a revolving arm, so that they all rotate horizontally about a fixed point on the ship deck. This will, however, result in a wider ship when sailing upwind, which may be problematic in narrow inlets and harbors. In addition, it will increase the cost of the wind turbine rig.

Noise from the wind turbine is not a problem, unless people are located directly under the wind turbine for long periods of time. Vestas lists the highest sound power level from the V90 turbine with a 65 m high tower, 10 m above ground, to 109.4 dBA, at 9 m/s. A person, 2 m tall, standing directly under the wind turbine, would then be located 8 m away from this

sound source. The sound pressure level received by the ear, is given by the formula

$$L_R = L_W - 10 \log(2\pi R^2) - \Delta L_a \quad (5.20)$$

where

L_R	is the sound pressure level of noise in dBA at distance R from the noise source
L_W	is the sound power level of the noise source(s) in dBA as given by Vestas
R	is the distance between the source and the receiver in meters
$\Delta L_a = \alpha_a R$	
α_a	is the attenuation of sound due to air absorption, in dBA/m. The value is dependent upon the sound frequency and spectral character of the sound. Here, α_a is taken to be 0.005 (Malcolm Hunt Associates, 2006).

Using Eq. 5.20, the person located directly under the wind turbine will perceive a sound of 83.3 dBA, which equals the noise on the roadside of a heavily trafficked highway. At a horizontal distance of 40 m from the wind turbine, a person would perceive a sound of 69 dBA, which equals soft radio music in homes.

A structural load and fatigue assessment of a Vestas V90 wind turbine on-board a ship is a study of its own, but in general, increasing ship size will result in lower accelerations. The wind turbine propelled ship should therefore be as large as possible to reduce accelerations, and hence stresses on the wind turbine, if not some form of hydraulic damping mechanism of the wind turbine is employed.

6 Conclusions and future perspectives

6.1 Conclusions

A method based on axial momentum theory has been outlined, in order to predict the steady-state speed of a wind turbine powered boat. This method is applied to a notional wind turbine powered catamaran, where the hull resistance is calculated with the computer program *Michlet*. The predicted steady-state boat speed is approximately 0.6 times the wind speed for true wind angles from directly upwind (0°) up to about 70° , regardless of the wind speed, when assuming calm water and a wind turbine efficiency of 0.4 for all wind speeds. The boat speed then decreases gradually down to about 0.44 times the wind speed, directly downwind. The predicted boat speed to wind speed ratio when the boat is sailing upwind is in good agreement with the results from testing of a similar full-scale wind turbine boat by Blackford (Blackford, 1985b), although Blackford's wind turbine boat was smaller than the theoretical one studied here. Results for other wind angles than directly upwind is not presented in (Blackford, 1985b), but the feature of higher boat speed upwind than downwind is also observed on the full-scale wind turbine powered catamaran *Revelation II*.

A related topic to wind turbine propulsion is the reversed configuration, where a water turbine is driving an air propeller. As shown by Bauer (Bauer, 1969) and Drela (Drela, 2009a,b), this configuration has the theoretical ability to propel a water vehicle faster than the wind, directly downwind. This configuration can also propel the boat slower than the wind, directly downwind, but vortex generation makes momentum theory invalid in this state, and this condition is therefore not studied further here. Based on a similar approach to the method of velocity prediction of wind turbine powered boats, design criteria with respect to water turbine efficiency and hydrofoil chord length, are set for a given hydrofoil boat in order to sail faster than the wind, directly downwind. The conclusion drawn from this is that practical design aspects such as size, weight, and material strength will make it difficult to construct such a boat, although the feature of sailing faster than the wind, directly downwind, is theoretically possible for a water vehicle.

Blackford's theory of optimal blade design for a wind turbine powered boat (Blackford, 1985a) has been presented and applied on a theoretical wind tur-

bine boat. Prandtl's tip loss factor and Goldstein factors have been applied in the blade design to correct for a finite number of blades, and it is shown that these correction factors influence mainly the chord length at radii near the wind turbine tip. Blackford also compared the net forward force from a wind turbine propulsor with a rigid airfoil, or wingsail, and concluded that wingsails contribute to more propulsive force than wind turbines per sail/-turbine disk area, when all wind angles are taken into consideration, for ship speed to wind speed ratios above about 0.5. The comparison with wingsail is done because, after wind turbine propulsion, wingsail is the form of wind-assisted propulsion that provides propulsive force for the broadest range of wind directions, as shown in Table 5.1.

Wind turbine propulsion of ships has been discussed. A notional wind turbine ship consisting of a 326 m L_{WL} VLCC carrying a Vestas V90 wind turbine for auxiliary propulsion, is set to sail a route across the North Sea in January. The wind turbine will save only 3.6% fuel compared to the ship sailing without the wind turbine, at a speed of 15 kn. However, if the ship speed is reduced to 10 kn, the fuel saving increases to 21.1%. This is mainly due to the fact that the total amount of fuel necessary to complete the journey in 10 kn is reduced by 54%, compared to that of 15 kn. It is shown that the stability of the wind turbine powered ship considered is good, and that noise from the wind turbine is not a problem. The height of such a ship, however, may be problematic.

Keeping the wind turbine radius at 90 m, Blackford's optimal blade design theory is applied to the notional wind turbine ship, in order to study its effect on the fuel saving. The optimized wind turbine has four blades, compared to the three-bladed Vestas V90 wind turbine, and its blades have over twice as high maximum chord length. Employing the optimized wind turbine on the VLCC results in slightly higher fuel saving than what is attained with the Vestas V90 wind turbine, for the route considered. The superiority of the optimized wind turbine design is made clearer when setting the wind turbine ship to sail only directly upwind. In this case, the optimized wind turbine would provide 30.8% of the required power, whereas the Vestas V90 would provide 23.8% of the required power, not taking the drag of the wind turbine tower into account in the calculations. The total propulsive efficiency is shown to be of tremendous influence on the fuel savings.

The consequence of this is that without accepting drastically decreasing transit speeds, a measure which will greatly reduce fuel consumption itself,

retrofitting existing vessels with a wind turbine for auxiliary propulsion is most beneficial for vessels with relatively slow cruising speeds compared to the wind speed. For a wind speed of 10 m/s, examples of such vessels are vessels with displacement hulls of length 10-15 m, which are limited by their hull length to speeds of about 4 m/s. Larger, slow sailing vessels may also benefit significantly from wind turbine propulsion. Bose and MacGregor (Bose and MacGregor, 1987) found that the yearly fuel savings resulting from the use of a 20 m diameter wind turbine onboard a 26 m long trawler was between 20% and 25%.

6.2 Future perspectives

As shown, neglecting the drag on the Vestas V90 wind turbine tower results in a fuel saving of 22.3%, compared to 21.1% when including the drag on the tower in the calculations, for the specific route and wind conditions considered here. The drag on the wind turbine tower of the optimized wind turbine is not studied here, due to the complexity of radially varying induced axial and tangential velocities in the blade element theory.

For more accurate results than those obtained with the blade element momentum theory, or the very simplified axial momentum theory, a CFD method such as a Reynolds-Averaged Navier Stokes (RANS) method should be used. This would in particular provide interesting results for the water vehicle propelled by an air propeller, working in the ring vortex state, where viscous effects are important. Using a RANS method, one can also calculate the complex flow through and behind the wind turbine in detail, in order to calculate the thrust on the wind turbine and the drag on the wind turbine tower more accurately.

Regarding the use of diffuser-augmented wind turbines (DAWTs) on ships for auxiliary propulsion, the increased drag due to the diffuser and supporting structure should be studied further, in order to conclude whether or not the increased power output exceeds the power to overcome the increased resistance.

Tougher demands on fuel consumption and emissions control will increase the focus on wind-assisted ship propulsion. Combining wind turbine propulsion

with other solutions, such as wingsails or kite, may be the solution for those environmentally friendly ships of the future that are bound to sail large parts of their routes against the wind.

References

- I. H. Abbott and A. E. von Doenhoff. *Theory of wing sections*. Dover Publications, 1959.
- K. Barry. Wind-Powered Car Travels Downwind Faster Than the Wind. *Wired*, June 2010. <http://www.wired.com/autopia/2010/06/downwind-faster-than-the-wind>. Retrieved, June 9, 2010.
- A. B. Bauer. Faster than the wind. In *Proceedings, First AIAA Symposium on the Aero/Hydronautics of Sailing*, 1969.
- BBC News. Design puts boat in a spin. http://news.bbc.co.uk/2/hi/uk_news/1507825.stm, August 2001. Retrieved, June 9, 2010.
- B. L. Blackford. Optimal blade design for windmill boats and vehicles. *Journal of Ship Research*, 29(2):139–149, 1985a.
- B. L. Blackford. Windmill thrusters: A comparison of theory and experient. *Journal of Wind Engineering and Industrial Aerodynamics*, 20:267–281, 1985b.
- J. Borton et al. Ride Like the Wind (only faster). <http://www.fasterthanthewind.org>, 2010. Retrieved, June 9, 2010.
- N. Bose. *Marine powering prediction and propulsors*. SNAME, 2008.
- N. Bose. Windmills - propulsion for a hydrofoil trimaran. In *Symposium on Wind Propulsion of Commercial Ships*. RINA, November 1980.
- N. Bose. The autogyro for ship propulsion. *International Shipbuilding Progress*, 30(348):179–186, 1983.
- N. Bose. Wind turbine drives - test results from the Falcon. *Journal of Wind Engineering and Industrial Aerodynamics*, 20:283–295, 1985.
- N. Bose and J. R. MacGregor. The use of a wind turbine for propulsive power generation aboard a Scottish Seiner/Trawler. *Wind Engineering*, 11 (1):38–50, 1987.
- N. Bose and J. A. Wilkinson. Performance tests on the wind turbine powered catamaran Revelation. *Wind Engineering*, 9 (1):9–23, 1985.
- J. Brix. *Manoeuvring Technical Manual*. Seehafen Verlag, 1993.

- J. Carlton. *Marine propellers and propulsion*. Elsevier Ltd., second edition, 2007.
- Discovery Channel. Daily Planet: May 04, 2010. <http://watch.discoverychannel.ca/daily-planet/may-2010/daily-planet---may-04-2010/#clip298008>, 2010. Retrieved, June 9, 2010.
- M. Drela. Dead-Downwind Faster Than The Wind (DDWFTTW) Analysis. Available at <http://www.mediafire.com/?xdmjm0von5q>, January 2009a. Retrieved, June 9, 2010.
- M. Drela. DDWFTTW Power Analysis . Available at <http://www.mediafire.com/?xbzbcyjy0b1>, January 2009b. Retrieved, June 9, 2010.
- EnergyBeta. <http://www.energybeta.com/wp-content/uploads/2009/06/giromill-232x300.jpg>, 2010. Retrieved, June 9, 2010.
- H. Glauert. *Division L of Aerodynamic Theory*. Durand Printing Committee, Calif. Institute of Technology, 1943.
- C. W. B. Grigson. A planar friction algorithm and its use in analysing hull resistance. *Trans. RINA*, pages 76–115, 2000.
- M. O. L. Hansen. *Aerodynamics of wind turbines*. Earthscan, 2008.
- Malcolm Hunt Associates. Assessment of environmental noise effects - ambient sound level monitoring & wind farm noise assessment. Technical Report 115-01-5(C), Meridian Energy Limited, July 2006. <http://www.meridianenergy.co.nz/NR/rdonlyres/88866D04-6373-49A3-8EA2-0DDA1939C115/0/AppendixINoiseReport.pdf>. Retrieved June 9, 2010.
- C. A. Marchaj. *Aero-Hydrodynamics of Sailing*. Dodd, Mead, 1964.
- J. H. Michell. The wave resistance of a ship. *Phil. Mag.*, 45(5):106–123, 1898.
- K. Minsaas and S. Steen. *Lecture notes: TMR4220 Naval hydrodynamics - Ship resistance*. Department of Marine Technology, Norwegian University of Science and Technology, 2008.
- D. Myrhaug. *TMR4230 Oceanography, Wind, Waves*. Department of Marine Technology, Norwegian University of Science and Technology, January 2006.

- C. T. Nance. Outlook for wind assistance. *Journal of Wind Engineering and Industrial Aerodynamics*, 19:1–17, 1985.
- D. G. Phillips. *An investigation on diffuser augmented wind turbine design*. PhD thesis, The University of Auckland, 2003.
- R. C. T. Rainey. The wind turbine ship. In *Symposium on Wind Propulsion of Commercial Ships*. RINA, November 1980.
- Renewable Energy UK. <http://www.reuk.co.uk/OtherImages/darrieus-rotor.jpg>, 2010. Retrieved, June 9, 2010.
- The green energy website. <http://www.thegreenenergywebsite.com/img/savonius3.jpg>, 2010. Retrieved, June 9, 2010.
- Vestas. Vestas V90 brochure. <http://www.autonavzduch.cz/dokumenty/vestasV90-3MW.pdf>. Retrieved, June 9, 2010.
- Vestas. Vestas V90 brochure. http://www.vestas.com/Files/Filer/EN/Brochures/Vestas_V_90-3MW-11-2009-EN.pdf, November 2009. Retrieved, June 9, 2010.
- Wikipedia. Wind turbine. http://en.wikipedia.org/wiki/Wind_turbine, 2010. Retrieved, June 9, 2010.
- Wind-Works. <http://www.wind-works.org/SmallTurbines/DuctedorAugmentedTurbines.html>, 2010. Retrieved, June 9, 2010.
- Windfinder. <http://www.windfinder.com>, 2010. Retrieved, June 9, 2010.

Appendix A Momentum theory

A.1 Momentum theory, wind turbine

The thrust on the wind turbine, also called the backward force on the wind turbine, if a wind turbine boat is sailing upwind, is equal to the time rate of change in momentum when the wind is slowed down by the wind turbine

$$F_W = \rho_a Q \Delta U \quad (\text{A.1})$$

where $Q = A_t U_t$ is the volume flow through the turbine disk of disk area A_t , and ΔU is the reduction in velocity in the turbine wake.

In the actuator disk theory, or axial momentum theory, it is assumed that there are no tangential velocities anywhere in the turbine stream, the blade number is infinite and that the flow velocity is uniformly distributed in the radial direction of the stream.

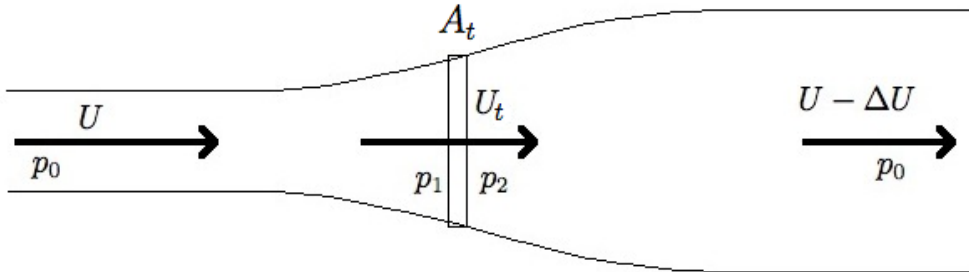


Figure A.1: Axial momentum theory, wind turbine.

First, we use Bernoulli's equation from far in front of the turbine to just in front of the turbine disk

$$\frac{\rho_a}{2} U^2 + p_0 = p_1 + \frac{\rho_a}{2} U_t^2 \quad (\text{A.2})$$

Bernoulli's equation from just behind the turbine disk to a point downstream in the wake yields

$$p_2 + \frac{\rho_a}{2} U_t^2 = p_0 + \frac{\rho_a}{2} (U - \Delta U)^2 \quad (\text{A.3})$$

The pressure jump across the turbine disk is then

$$\Delta p = p_1 - p_2 = \rho_a \Delta U \left(U - \frac{\Delta U}{2} \right) \quad (\text{A.4})$$

The thrust can also be expressed as the difference in pressure across the disk multiplied with the disk area

$$F_W = A_t \Delta p \quad (\text{A.5})$$

$$F_W = \rho_a Q \Delta U = \rho_a \Delta U \left(U - \frac{\Delta U}{2} \right) A_t \quad (\text{A.6})$$

From this we see that the volume flow through the turbine disk is

$$Q = A_t \left(U - \frac{\Delta U}{2} \right) \quad (\text{A.7})$$

and that the corresponding velocity through the disk is

$$U_t = U - \frac{\Delta U}{2} = U(1 - a) \quad (\text{A.8})$$

where a is the fractional decrease of the wind velocity at the propeller disk, also known as the axial induction factor. The reduction in the wind velocity in the wake is as noted above ΔU , which, by use of a , can be written $\Delta U = 2Ua$.

Looking at a fluid annulus of width dr , the backward force can be found by replacing Q with $2\pi r U(1 - a)$ and ΔU with $2Ua$ in Eq. A.1. If the apparent wind has an angle θ' to the boat course, see Fig. 2.5, the component of the backward force in the direction of the boat course is

$$dF_W = 4\rho_a U^2 a(1 - a)\pi r dr \cos \theta' \quad (\text{A.9})$$

If we assume that there are no tangential velocities in the inflow to the turbine, whereas in the wake, the tangential velocity is $2a'\Omega r$, the torque, dQ , that acts on a fluid annulus of width dr , is equal to the time rate of change of angular momentum of the annulus, as it flows through the turbine

$$dQ = dm r 2a'\Omega r \quad (\text{A.10})$$

where the mass flow of the fluid annulus is given as

$$d\dot{m} = \rho_a 2\pi r dr U(1 - a) \quad (\text{A.11})$$

which yields

$$dQ = U(1 - a)4\pi a' \Omega r^3 \rho_a dr \quad (\text{A.12})$$

Consider the ratio dQ/dF_W , where dQ is written as in Eq. 4.7 and as Eq. 4.8, and dF_W is written as Eq. 4.4 and as Eq. 4.6:

$$\frac{dQ}{dF_W} = \frac{\frac{1}{2}\rho_a c N V^2 C_L (\sin \phi - \epsilon \cos \phi) r dr}{\frac{1}{2}\rho_a c N V^2 (C_L \cos \phi + C_D \sin \phi) dr \cos \theta'} = \frac{U(1 - a)4\pi a' \Omega r^3 \rho_a dr}{4\rho_a U^2 a(1 - a)\pi r dr \cos \theta'} \quad (\text{A.13})$$

which can be simplified to

$$\frac{\sin \phi - \epsilon \cos \phi}{\cos \phi + \epsilon \sin \phi} = \frac{\Omega r a'}{U a} \quad (\text{A.14})$$

using $\epsilon = C_D/C_L$. By using Eq. 4.12 and Fig. 4.1, this reduces to a quadratic equation between a and a' , whose solution is

$$a'(s) = -\frac{1}{2}(1 + \epsilon/s) + \frac{1}{2}\sqrt{(1 + \epsilon/s)^2 + 4a[(1 - a)/s^2 - \epsilon/s]} \quad (\text{A.15})$$

A.2 Momentum theory, propeller

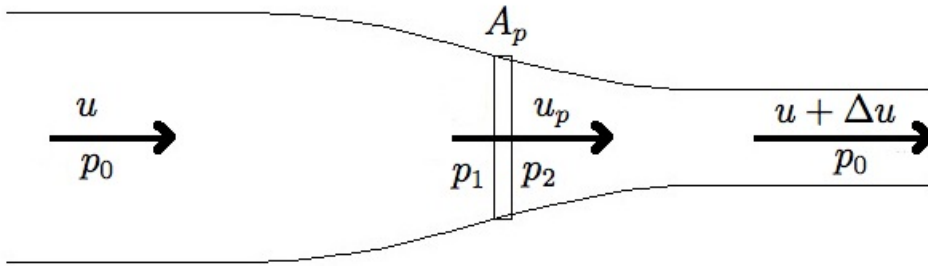


Figure A.2: Axial momentum theory, propeller.

Axial momentum theory applied for the propeller also assumes that there are no tangential velocities anywhere in the propeller stream, that the blade

number is infinite and that the flow velocity is uniformly distributed in the radial direction of the stream. The fluid is accelerated from velocity u in front of the propeller, to u_p at the propeller disk, and to $u_e = u + \Delta u$ in the propeller wake. If we redo the analysis for the wind turbine in Appendix A.1, for the propeller case, we find that the thrust on the propeller is

$$F = \rho_w Q \Delta u = \rho_w A_p \frac{u_e + u}{2} (u_e - u) = \rho_w A_p \frac{u_e^2 - u^2}{2} \quad (\text{A.16})$$

$$\Rightarrow \left(\frac{u_e}{u} \right)^2 = \frac{F}{A_p u^2 \frac{\rho_w}{2}} + 1 \quad (\text{A.17})$$

and that the velocity through the propeller disk is $u_p = (u_e + u)/2$, which inserted into A.17 gives

$$\frac{u_p}{u} = \frac{1}{2} \left[\frac{F}{A_p u^2 \frac{\rho_w}{2}} + 1 \right]^{1/2} + \frac{1}{2} \quad (\text{A.18})$$

The ideal (minimum) power required to drive the propeller is then

$$P_i = F u_p = \frac{1}{2} F u \left[\left(\frac{F}{A_p u^2 \frac{\rho_w}{2}} + 1 \right)^{1/2} + 1 \right] \quad (\text{A.19})$$

whereas the propulsive power is

$$P = F u \quad (\text{A.20})$$

The ideal efficiency is then

$$\eta_i = \frac{P}{P_i} = \frac{2}{1 + \left(\frac{F}{A_p u^2 \frac{\rho_w}{2}} + 1 \right)^{1/2}} \quad (\text{A.21})$$

A.3 Propeller efficiency at zero speed

The usual definition of propeller efficiency

$$\eta_p = \frac{F V_A}{P_D} \quad (\text{A.22})$$

where F is the propeller thrust, V_A is the advance number, and P_D is the power delivered to the propeller, is only meaningful when the advance velocity is non-zero. When the advance velocity is zero, the propeller efficiency is zero according to this definition, regardless of the relation between thrust and power. A relation between thrust and power when the advance velocity is zero can be found from the following:

The power supplied to the water is

$$P = \frac{1}{2} \rho_w A_p (\Delta u)^3 \quad (\text{A.23})$$

The ideal thrust is

$$F_0 = \rho_w A_p (\Delta u)^2 \quad (\text{A.24})$$

which gives the following expression for the induced velocity:

$$\Delta u = \sqrt{\frac{F_0}{\rho_w A_p}} = \left[\frac{2P}{\rho_w A_p} \right]^{1/3} \quad (\text{A.25})$$

The relation between thrust and power can then be expressed as

$$F_0 = \rho_w A_p \left[\frac{2P}{\rho_w A_p} \right]^{2/3} \quad (\text{A.26})$$

or

$$F_0 = [4\rho_w A_p P^2]^{1/3} \quad (\text{A.27})$$

where P is power supplied to the fluid. If the term ‘‘pump efficiency’’ $\eta_{p0} = P/P_D$ is introduced, the power supplied to the propeller is

$$F_0 = (\rho_w \pi \eta_{p0}^2)^{1/3} (D^2 P_D^2)^{1/3} \quad (\text{A.28})$$

MARINTEK has found from bollard pull model tests that η_{p0} is typically around 0.45 for open propellers.

Appendix B Resistance and hydrostatics results, ShipX

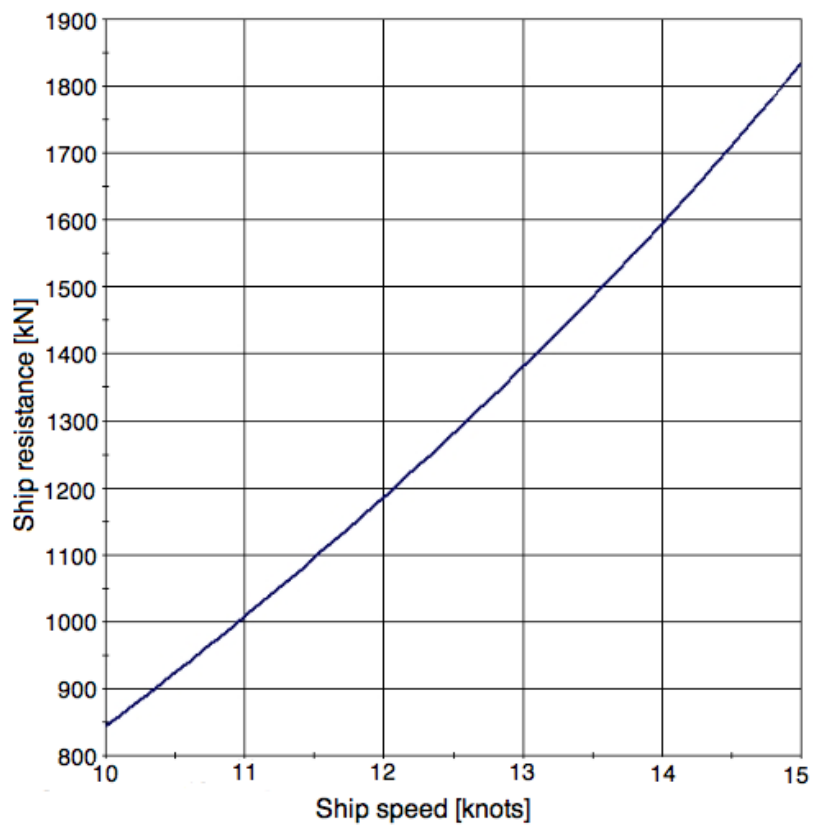



Figure B.1: Resistance curve for the VLCC from ShipX.

	HYDROSTATICS		ENCL.
			REPORT
			DATE 2010-05-10
			REF

SHIP: **KVLCC2 - Added resistance tests**
 Loading condition: Design WL
 Draught AP/FP: 20.800 / 20.800 [m]

	Symbol	Unit	
Length overall	L _{OA}	[m]	333.500
Length betw. perp.	L _{PP}	[m]	320.000
Breadth moulded	B	[m]	58.001
Depth to 1 st deck	D	[m]	28.015
Draught at L _{PP} /2	T	[m]	20.800
Draught at FP	T _{FP}	[m]	20.800
Draught at AP	T _{AP}	[m]	20.800
Trim (pos. aft)	t	[m]	0.000
Rake of keel		[m]	0.000
Rise of floor		[m]	0.000
Bilge radius		[m]	0.000
Sea water density	ρ_s	[kg/m ³]	1025.00
Shell plating thickness		[mm]	0
Shell plating in % of displ.		[%]	0.50
Length on waterline	L _{WL}	[m]	325.503
Breadth waterline	B _{WL}	[m]	58.001
Volume displacement	∇	[m ³]	312693.3
Displacement	Δ	[t]	322113.2
Prismatic coefficient*	C _P	[-]	0.8116
Block coefficient*	C _B	[-]	0.8100
Midship section coefficient	C _M	[-]	0.9979
Longitudinal C.B. from L _{PP} /2	LCB	[m]	11.177
Longitudinal C.B. from L _{PP} /2*	LCB	[% L _{PP}]	3.493
Longitudinal C.B. from AP	LCB	[m]	171.177
Vertical C.B.	VCB	[m]	10.873
Wetted surface	S	[m ²]	27813.86
Wetted surface of transom stern	A _T	[m ²]	13.56
Waterplane area	A _W	[m ²]	16737.50
Waterplane area coefficient	C _W (L _{WL})	[-]	0.887
Longitudinal C.F. from L _{PP} /2	LCF	[m]	0.060
Longitudinal C.F. from AP	LCF	[m]	160.060
Immersion	DP ₁	[t/cm]	171.559
Trim moment	MT ₁	[t · m/cm]	3881.672
Transverse metacenter above keel	KM _T	[m]	24.306
Longitudinal metacenter above keel	KM _L	[m]	387.549

Remarks: *Refers to L_{PP}
 Hydrostatic corrections not included